

Singular ring solutions of critical and supercritical nonlinear Schrödinger equations

Gadi Fibich^{a,*}, Nir Gavish^a, Xiao-Ping Wang^b

^a School of Mathematical Sciences, Tel Aviv University, Tel Aviv 69978, Israel

^b Department of Mathematics, The Hong Kong University of Science and Technology, Clear Water Bay, Kowloon, Hong Kong

Received 17 September 2006; received in revised form 18 April 2007; accepted 30 April 2007

Available online 6 May 2007

Communicated by J. Lega

Abstract

We present new singular solutions of the nonlinear Schrödinger equation (NLS)

$$i\psi_t(t, r) + \psi_{rr} + \frac{d-1}{r}\psi_r + |\psi|^{2\sigma}\psi = 0, \quad 1 < d, \frac{2}{d} \leq \sigma \leq 2.$$

These solutions collapse with a quasi self-similar ring profile ψ_Q , i.e. $\psi \sim \psi_Q$, where

$$\psi_Q = \frac{1}{L^{1/\sigma}(t)} Q \left(\frac{r - r_m(t)}{L} \right) \exp \left[i \int_0^t \frac{ds}{L^2(s)} + i \frac{L_t}{4L} \left[\alpha r^2 + (1 - \alpha)(r - r_m(t))^2 \right] \right],$$

$L(t)$ is the ring width that vanishes at the singularity, $r_m(t) = r_0 L^\alpha(t)$ is the ring radius and $\alpha = \frac{2-\sigma}{\sigma(d-1)}$. The blowup rate of these solutions is $\frac{1}{1+\alpha}$ for $\frac{2}{d} \leq \sigma < 2$ and $1 < d$ ($0 < \alpha \leq 1$), and a square root with a loglog correction (the loglog law) when $\sigma = 2$ and $1 < d$ ($\alpha = 0$). Therefore, the NLS has solutions that collapse with any blowup rate p for $1/2 \leq p < 1$. This study extends the results of [G. Fibich, N. Gavish, X. Wang, New singular solutions of the nonlinear Schrödinger equation, *Physica D* 211 (2005) 193–220] for $\sigma = 1$ and $d = 2$, and of [P. Raphael, Existence and stability of a solution blowing up on a sphere for a L^2 super critical non linear Schrödinger equation, *Duke Math. J.* 134 (2) (2006) 199–258] for $\sigma = 2$ and $d = 2$, to all $2/d \leq \sigma \leq 2$ and $1 < d$.

© 2007 Elsevier B.V. All rights reserved.

Keywords: Nonlinear Schrödinger equation; Supercritical collapse; Self-similar solution; Singularity; Collapse; Ring profile; Blowup rate

1. Introduction

1.1. Brief review of NLS theory

The focusing nonlinear Schrödinger equation (NLS)

$$i\psi_t(t, \mathbf{x}) + \Delta\psi + |\psi|^{2\sigma}\psi = 0, \quad \psi(0, \mathbf{x}) = \psi_0(\mathbf{x}), \quad (1)$$

where $\mathbf{x} = (x_1, x_2, \dots, x_d)$ and $\Delta = \partial_{x_1 x_1} + \dots + \partial_{x_d x_d}$, is one of the canonical nonlinear equations in physics, arising

in various fields such as nonlinear optics, plasma physics, Bose–Einstein condensates (BEC), and surface waves. We now briefly review NLS theory, for more information, see [1–3]. The NLS (1) has two important conservation laws: *power* (L^2 norm) conservation

$$P(t) = \int |\psi|^2 dx \equiv P(0), \quad (2)$$

and Hamiltonian conservation

$$H(t) = \int |\nabla\psi|^2 dx - \frac{1}{\sigma+1} \int |\psi|^{2\sigma+2} dx \equiv H(0). \quad (3)$$

The NLS is called *subcritical* if $\sigma d < 2$. In this case, all solutions exist globally. In contrast, solutions of the

* Corresponding address: Department of Applied Mathematics, Tel Aviv University, Tel Aviv 69978, Israel.

E-mail addresses: fibich@tau.ac.il (G. Fibich), nirgvsh@tau.ac.il (N. Gavish), mawang@ust.hk (X.-P. Wang).

URL: <http://www.math.tau.ac.il/~fibich> (G. Fibich).

critical ($\sigma d = 2$) and supercritical ($\sigma d > 2$) NLS can become singular in finite time T_c , i.e.

$$\lim_{t \rightarrow T_c} \|\psi\|_{H^1} = \infty, \quad 0 < T_c < \infty,$$

where

$$\|\psi\|_{H^1} = \sqrt{\int |\psi|^2 dx + \int |\nabla \psi|^2 dx}.$$

1.1.1. Critical NLS ($\sigma d = 2$)

We now review the theory of singular solutions of the critical NLS. Since $\sigma = 2/d$, the critical NLS can be written as

$$i\psi_t(t, \mathbf{x}) + \Delta \psi + |\psi|^{4/d} \psi = 0, \quad \psi(0, \mathbf{x}) = \psi_0(\mathbf{x}). \quad (4)$$

The critical NLS (4) has waveguide solutions of the form $\psi = e^{it} R(r)$, where $r = |\mathbf{x}|$ and R is the solution of

$$R''(r) + \frac{d-1}{r} R' - R + R^{4/d+1} = 0$$

$$R'(0) = 0, \quad R(\infty) = 0. \quad (5)$$

When $d \geq 2$, Eq. (5) has an enumerable number of solutions $\{R^{(n)}\}_{n=0}^{\infty}$, which can be arranged in order of increasing power [4], i.e.

$$\int (R^{(0)})^2 dx \leq \int (R^{(1)})^2 dx \leq \int (R^{(2)})^2 dx \leq \dots$$

Of most importance is the ground state solution $R := R^{(0)}$, also known in the case $d = 2$ as the *Townes profile* [5]. The ground state R attains its maximum at $r = 0$, and is monotonically decreasing for $0 \leq r < \infty$.

As noted, solutions of the critical NLS (4) can self-focus and become singular at a finite time T_c . A necessary condition for singularity formation is that the *initial power* $P(0)$ exceeds the critical power P_{cr} , i.e. $P(0) \geq P_{cr}$, where P_{cr} is equal to power of the ground state R , i.e. $P_{cr} = \int R^2 dx$ [6]. A sufficient condition for collapse is that the Hamiltonian is negative, i.e. $H(0) < 0$.

The critical NLS (4) is invariant under the following lens (pseudo-conformal) transformation [7]. Let $\psi(t, \mathbf{x})$ be a solution of the NLS (4), and let

$$\tilde{\psi}(t, \mathbf{x}) = \frac{1}{L^{1/\sigma(t)}} \psi\left(\tau, \frac{\mathbf{x}}{L}\right) \exp\left(i \frac{L_t}{4L} |\mathbf{x}|^2\right),$$

$$\tau = \int_0^t \frac{ds}{L^2(s)}, \quad (6)$$

where $L(t) = f_c(T_c - t)$, f_c is a positive constant and $\sigma = 2/d$. Then, $\tilde{\psi}(t, \mathbf{x})$ is also a solution of the NLS (4). Applying the lens transformation (6) to the waveguide solutions $\psi = e^{it} R^{(n)}(r)$, where $R^{(n)}$ are the solutions of (5), gives rise to the explicit blowup solutions

$$\psi_{ex}^{(n)}(t, r) = \frac{1}{L^{1/\sigma(t)}} R^{(n)}\left(\frac{r}{L}\right) e^{i\tau + i \frac{L_t}{4L} r^2},$$

$$\tau = \int_0^t \frac{ds}{L^2(s)}, \quad L(t) = f_c(T_c - t), \quad (7)$$

that become singular at $t = T_c$. These explicit blowup solutions, however, are unstable.

Numerical studies conducted during the 1980s (see e.g., [8, 9]) suggested that stable singular solutions of the critical NLS (4) collapse with the universal, radially-symmetrical asymptotic profile ψ_R . Thus, regardless of the initial condition, near the singularity $\psi \sim \psi_R$, where

$$\psi_R(t, r) = \frac{1}{L^{1/\sigma(t)}} R\left(\frac{r}{L}\right) e^{i\tau + i \frac{L_t}{4L} r^2}, \quad \tau = \int_0^t \frac{ds}{L^2(s)}, \quad (8)$$

R is the ground-state solution of (5) and $\lim_{t \rightarrow T_c} L(t) = 0$. More precisely, it turned out that only the inner core of the solution collapses into the singularity with the asymptotic profile ψ_R , while the rest of the solution remains in L^2 , i.e.

$$\psi \sim \begin{cases} \psi_R & 0 \leq r \leq \kappa L(t) \\ \psi_{outer} & \kappa L(t) < r, \end{cases} \quad (9)$$

where $\kappa \gg 1$.

The understanding that NLS collapse is quasi self-similar with the universal self-similar profile ψ_R was crucial for the derivation of the blowup rate of the critical NLS, which turned out to be a square root with a loglog correction (the *loglog law*) [10–13], i.e.

$$L(t) \sim \left(\frac{2\pi(T_c - t)}{\log \log 1/(T_c - t)} \right)^{\frac{1}{2}}, \quad t \rightarrow T_c. \quad (10)$$

The convergence to ψ_R was also at the heart of the derivation of the asymptotic theory for the effects of small perturbations in the critical NLS, known as *modulation theory* [1]. A rigorous proof of the convergence to the self-similar profile ψ_R , however, turned out to be a hard problem. Partial results were obtained by Weinstein [14] and by Nawa [15,16]. Only in 2003, however, Merle and Raphael proved that all singular solutions of the critical NLS (4) with power moderately above P_{cr} collapse with the asymptotic ψ_R profile at the loglog blowup rate [17], and see also [18–20]. Concurrently, Moll, Gaeta and Fibich demonstrated experimentally that the profile of collapsing laser beams is given by the R profile [21]. Therefore, all the rigorous, asymptotic, numerical and experimental evidence until 2005 suggested that *all* stable singular solutions of the critical NLS collapse with the ψ_R profile.

1.1.2. Supercritical NLS ($\sigma d > 2$)

In contrast to the extensive theory on singular solutions of the critical NLS, much less is known about singular solutions of the supercritical NLS. Numerical simulations carried out during the 1980s (see, e.g. [22–24]) showed that solutions of the supercritical NLS collapse with a self-similar asymptotic profile ψ_S , i.e. $\psi \sim \psi_S$, where

$$\psi_S(t, r) = \frac{1}{L^{1/\sigma}} S\left(\frac{r}{L}\right) e^{i\tau + i \frac{L_t}{4L} r^2}, \quad \tau = \int_0^t \frac{ds}{L^2(s)}. \quad (11)$$

The blowup rate of these solutions turned out to be a square root, i.e.

$$L(t) \sim f_c \sqrt{T_c - t}, \quad t \rightarrow T_c, \quad (12)$$

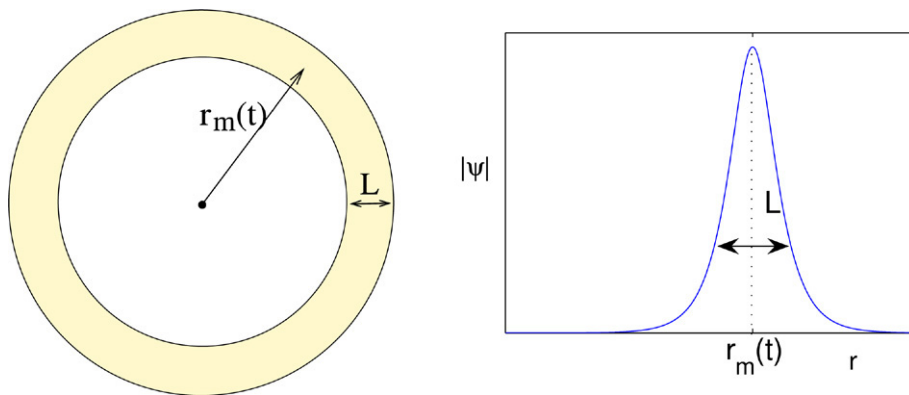


Fig. 1. Illustration of ring radius $r_m(t)$ and width $L(t)$.

where $f_c > 0$. In addition, the self-similar profile S is the solution of

$$S''(r) + \frac{d-1}{r} S' - S + |S|^{2\sigma} S + \left(\frac{f_c^4}{16} r^2 - i \frac{f_c^2(\sigma d - 2)}{4} \right) S = 0, \quad (13)$$

$$S'(0) = 0, \quad S(\infty) = 0.$$

As in the critical case, $|S|$ attains its maximum at $r = 0$, and is monotonically decreasing for $0 \leq r < \infty$. The self-similar profile ψ_S involves a complicated nonlinear eigenvalue problem which is not fully understood. Therefore, unlike the critical case, the theory of singular solutions of the supercritical NLS lacks a rigorous basis at present.

1.2. Singular ring solutions

As we have seen, until 2005 all known stable singular solutions of the critical and supercritical NLS collapsed with the ψ_R and ψ_S profiles, respectively.¹ Since the maximum of R and S is attained at $r = 0$, and since they decrease monotonically for $0 \leq r < \infty$, we will refer to ψ_R and ψ_S as *singular peak solutions*.

In 2005, we presented the first singular nonpeak solutions of the NLS, for the radially-symmetrical two-dimensional cubic critical NLS ($\sigma = 1, d = 2$)

$$i\psi_t(t, r) + \psi_{rr} + \frac{1}{r}\psi_r + |\psi|^2\psi = 0, \quad (14)$$

see [26]. These solutions have the asymptotic self-similar ring profile ψ_G , i.e. $\psi(t, r) \sim \psi_G(t, r)$, where

$$\psi_G(t, r) = \frac{1}{L(t)} G(\rho) e^{i\tau + i\frac{L}{4t}r^2}, \quad (15)$$

$$\tau = \int_0^t \frac{ds}{L^2(s)}, \quad \rho = \frac{r}{L}.$$

The profile G is the solution of

$$G''(\rho) + \frac{G'}{\rho} + \left[\frac{f_c^4}{16} \rho^2 - 1 \right] G + G^3 = 0,$$

$$G'(0) = 0, \quad G(\infty) = 0,$$

and has a ring shape, i.e. it attains its global maximum at some $\rho_m > 0$ and decreases monotonically away from ρ_m . Therefore, ψ_G is a singular *ring* profile and not a singular peak solution. The blowup rate of ψ_G is different from that of ψ_R , as it is a square root with no loglog correction. Numerical simulations suggested that the ψ_G profile is a stable solution of the radially-symmetrical NLS (14). Since, however, the G -profile has an infinite L^2 norm, it is still an open issue whether the ring profile is maintained all the way up to the singularity (see Section 1.4).

In 2006, Raphael [27] discovered and rigorously proved the existence and stability of singular ring solutions of the radially-symmetrical supercritical two-dimensional quintic NLS ($\sigma = 2, d = 2$)

$$i\psi_t(t, r) + \psi_{rr} + \frac{1}{r}\psi_r + |\psi|^4\psi = 0. \quad (16)$$

These singular solutions have the asymptotic self-similar profile $\psi(t, r) \sim \psi_P(t, r)$, where²

$$\psi_P(t, r) \sim \frac{1}{L^{1/2}(t)} P(\rho) e^{i\tau(t)}, \quad \rho = \frac{r - r_m(t)}{L(t)}, \quad (17)$$

$P(\rho) = \sqrt[4]{3} \operatorname{sech}^{\frac{1}{2}}(2\rho)$, $r_m(t)$ is the ring radius, i.e. the location of the ring peak, and $L(t)$ is the ring width, see Fig. 1. Since $r_m(t) > 0$, ψ_P is a self-similar *ring* profile. The blowup rate of ψ_P is a square root with a loglog correction, i.e. the loglog law (10). A unique feature of ψ_P is that the collapsing ring is *standing*, i.e. the ring's radius approaches a positive constant as the solution collapses

$$\lim_{t \rightarrow T_c} r_m(t) = r_m(T_c) > 0.$$

Therefore, ψ_P is different from all previously known singular peak and ring solutions of the NLS, since it blows up on a sphere $r = r_m(T_c) > 0$, whereas ψ_R , ψ_S and ψ_G collapse at a point (or, at most at, a finite number of isolated points [28]).

¹ In [25], Budd showed that Eq. (13) also gives rise to ring (multibump) solutions of the supercritical NLS. The corresponding ψ_S profile, however, turned out to be unstable.

² This form of ψ_P is the one stated in Theorem 1 in [27].

1.3. Main results

As seen in Section 1.2, until now there have been two “isolated” cases of singular ring solutions of the NLS: ψ_G in the critical case $d = 2$, $\sigma = 1$, and ψ_P in the supercritical case $d = 2$, $\sigma = 2$. In this study, we show that these two ring solutions belong to a new family of ring solutions of the radially-symmetrical NLS equations

$$i\psi_t(t, r) + \psi_{rr} + \frac{d-1}{r}\psi_r + |\psi|^{2\sigma}\psi = 0, \quad (18a)$$

where

$$2/d \leq \sigma \leq 2, \quad 1 < d. \quad (18b)$$

These new ring solutions were first observed in [26], where we presented preliminary simulations of the supercritical three dimensional cubic NLS ($\sigma = 1$, $d = 3$)

$$i\psi_t(t, r) + \psi_{rr} + \frac{2}{r}\psi_r + |\psi|^2\psi = 0, \quad (19)$$

that collapse with a ring profile ψ_Q , which is different from the asymptotic ring profiles ψ_G and ψ_P . Indeed, in the case of ψ_G , the ring radius satisfies $r_m(t) = \rho_m L(t)$. Therefore, ψ_G undergoes *equal-rate collapse*, i.e. the ring radius and the ring width go to zero at the same rate. In the case of ψ_P , the collapsing ring is standing, i.e. $r_m(t) \approx r_m(T_c) > 0$. In contrast, we have seen in [26] that for the supercritical ring solution of (19), $r_m(t) \sim r_0 L^p(t)$ where $p \approx 1/2$. Therefore ψ_Q does not undergo equal rate collapse, nor is it a collapsing standing ring. Hence, the asymptotic profile ψ_Q is different from ψ_G and from ψ_P .³

In order to find the new asymptotic profile ψ_Q , we first note that $r_m = r_0 L(t)$, $r_m \approx r_0 L^{1/2}(t)$, and $r_m \approx r_0$ for ψ_G , ψ_Q and ψ_P , respectively. Therefore, ψ_Q is “somewhere between” ψ_G and ψ_P . In order to “interpolate” the ring radius $r_m(t)$ between ψ_G and ψ_P , we set $r_m(t) = r_0 L^\alpha(t)$, so that $\alpha = 1$ correspond to the equal-rate profile ψ_G and $\alpha = 0$ corresponds to the standing ring profile ψ_P .

The next step in our analysis is to note that ψ_P is given by

$$\psi_P(t, r) = \frac{1}{L^{1/2}(t)} P(\rho) e^{i\tau(t) + i\frac{L}{4t}(r-r_m(t))^2},$$

$$\rho = \frac{r - r_m(t)}{L(t)}. \quad (20)$$

This expression differs from the one in Theorem 1 of [27], see Eq. (17), by the quadratic radial phase term. This term goes to zero as $t \rightarrow T_c$, which is why it did not appear in Theorem 1 of [27]. Nevertheless, this radial phase term will be vital for our analysis of the supercritical ring solutions.

Next, we construct the new asymptotic ring profile ψ_Q by “interpolating” the asymptotic profile of ψ_G and of ψ_P as follows:

³ After this paper was submitted, we found out that collapsing ring solutions of the 3D cubic NLS (19) were already observed by Degtiarev, Zakharov and Rudakov [29].

Proposition 1. Eq. (18) has singular ring solutions whose asymptotic profile is given by

$$\psi_Q = \frac{1}{L^{1/\sigma}(t)} Q(\rho) e^{i\tau + i\alpha\frac{L}{4t}r^2 + i(1-\alpha)\frac{L}{4t}(r-r_m(t))^2}, \quad (21a)$$

where

$$\tau = \int_0^t \frac{ds}{L^2(s)}, \quad \rho = \frac{r - r_m(t)}{L}, \quad r_m(t) = r_0 L^\alpha(t). \quad (21b)$$

Proof. This result follows from Eq. (63) and from Propositions 4, 16 and 23. \square

The new asymptotic profile ψ_Q has a two radial phase terms. This is different from all previously known asymptotic NLS profiles, which have a single radial phase term. In order to understand the meaning of this new feature, we note that the quadratic phase term centered at $r = 0$ corresponds to focusing towards the origin, and the quadratic phase term centered at $r = r_m(t)$ corresponds to focusing towards $r_m(t)$. The blowup behaviour of ψ_Q is, therefore, a combination of “global” ring focusing towards the origin, together with ring width shrinking towards $r_m(t)$.

The parameter α defines the relation between the ring radius $r_m(t)$ and the ring width $L(t)$. The admissible values of α are (Lemma 8)

$$0 \leq \alpha \leq 1.$$

The relation between α and (σ, d) is given in the following proposition:

Proposition 2. Let ψ be a singular ring solution of the NLS (18) with an asymptotic blowup profile $\psi(t, r) \sim \psi_Q(t, r)$, where ψ_Q is given by (21). Then

$$\alpha = \frac{2 - \sigma}{\sigma(d - 1)}. \quad (22)$$

Proof. This follows from Lemmas 12, 18 and 20. \square

Therefore, $\alpha = 1$ (i.e. equal-rate collapse) if and only if $\sigma d = 2$, $\alpha = 0$ (i.e. standing ring collapse) if and only if $\sigma = 2$, and $0 < \alpha < 1$ if and only if $2/d < \sigma < 2$.

The blowup rate of ψ_Q is as follows:

Proposition 3. Let ψ be a singular ring solution of the NLS (18) with an asymptotic blowup profile $\psi(t, r) \sim \psi_Q(t, r)$, where ψ_Q is given by (21). Then, the blowup rate is given by

$$L(t) \sim \begin{cases} (T_c - t)^{\frac{1}{1+\alpha}}, & \frac{2}{d} \leq \sigma < 2, \quad (0 < \alpha \leq 1), \\ \sqrt{\frac{2\pi(T_c - t)}{\log \log \frac{1}{T_c - t}}}, & \sigma = 2, \quad (\alpha = 0). \end{cases} \quad (23)$$

Proof. This follows from Propositions 4, 16 and 23. \square

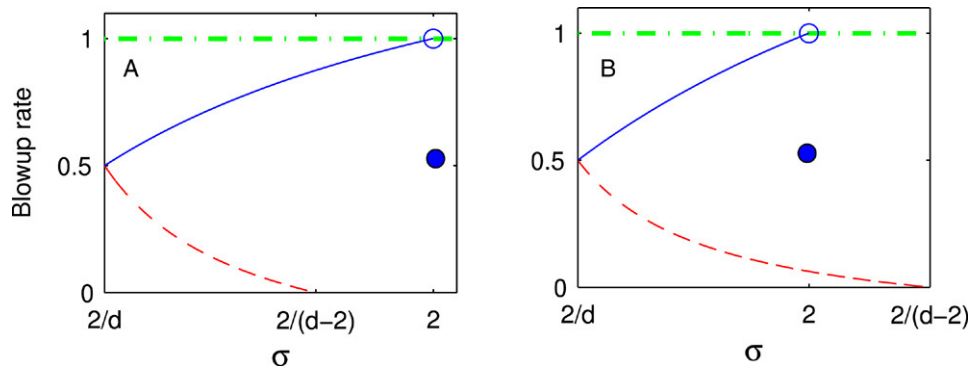


Fig. 2. Blowup rate p of the collapsing ring solutions is equal to $\frac{1}{1+\alpha}$ for $2/d \leq \sigma < 2$ (solid) and to $1/2$ (ignoring the loglog correction) for $\sigma = 2$ (full circle). Dashed curve is the rigorous lower bound (24), dash-dotted curve is the rigorous upper bound (26). A: $1 < d < 3$. B: $3 < d$.

As noted, until this study all known stable NLS singular solutions collapsed with either a square-root blowup rate or a square-root blowup rate with a loglog correction. Since $1/(1 + \alpha)$ assumes the values $[1/2, 1)$, Proposition 3 shows that the NLS can have singular ring solutions with any blowup rate p , $1/2 \leq p < 1$. In addition, it shows that there is a continuous transition between the blowup rate of singular ring solutions of the critical and the supercritical NLS (i.e. as $\sigma d \rightarrow 2+$). This continuity is exactly the opposite from singular peak solutions, where there is a discontinuity between the loglog law blowup rate (10) of the critical NLS, and the square root blowup rate (12) of the supercritical NLS. Proposition 3 also shows that there is a discontinuity in the blowup rate at $\sigma = 2$. Indeed, $L(t; \sigma \rightarrow 2-, d) \sim f_c \cdot (T_c - t)$, whereas

$$L(t; \sigma = 2, d) \sim \sqrt{\frac{2\pi(T_c - t)}{\log \log \frac{1}{T_c - t}}}.$$

The discontinuity at $\sigma = 2$ is also exactly the opposite from a singular peak solution, since the supercritical peak solutions have a square root blowup rate for all $\sigma d > 2$.

Cazenave and Weissler [30] proved that the blowup rate⁴ of the NLS (18a) is bounded by

$$L(t) \leq M(T_c - t)^{\frac{1}{2} - \frac{\sigma d - 2}{4\sigma}}, \quad 2 < d, \frac{2}{d} \leq \sigma < \frac{2}{d-2}. \quad (24)$$

According to Proposition 3, the blowup rate of the singular ring solutions is given by $\frac{1}{1+\alpha}$ for $\frac{2}{d} \leq \sigma < 2$. Since,

$$\underbrace{\frac{1}{2} - \frac{\sigma d - 2}{4\sigma}}_{(24)} \leq \frac{1}{2} \leq \underbrace{\frac{1}{1+\alpha}}_{(23)} = \frac{1}{2} + \frac{\sigma d - 2}{2(2 + \sigma d - 2\sigma)}, \quad (25)$$

the $\frac{1}{1+\alpha}$ blowup rate is consistent with the rigorous bound (24). The two inequalities in (25) are equalities only for $\sigma d = 2$. Hence, the bound (24) is sharp only in the critical case. The rigorous bound (24) is monotonically decreasing in σd ,

whereas the blowup rate is monotonically increasing in σd . Therefore, as σd increases the gap between the $\frac{1}{1+\alpha}$ blowup rate and the rigorous bound increases, see Fig. 2.

Let $J[\theta] = \int_0^{T_c} \|\nabla \psi(t)\|_2^\theta dt$. Merle [31] proved that for blowup solutions of the supercritical NLS, $J[\theta] < \infty$ for $\theta < 1$ and infinite for $\theta > \theta_2 = 4\sigma/(2\sigma + 2 - d\sigma)$. This implies that the blowup rate p is bounded by

$$p < 1. \quad (26)$$

Until now, numerical simulations (of peak-type supercritical solutions) suggested that the upper bound (26) is very crude. Our results show that, in fact, this bound is sharp, in the sense that for any $0 < \epsilon \ll 1$, there exist NLS blowup solutions with blowup rate $p = 1 - \epsilon$. (see Fig. 2).

In the supercritical case $2/d < \sigma \leq 2$, the quasi self-similar profile Q , see Proposition 1, is given by

$$Q(\rho; \sigma) = \omega^{\frac{1}{\sigma}} (1 + \sigma)^{\frac{1}{2\sigma}} [\text{sech}(\omega\sigma\rho)]^{\frac{1}{\sigma}}, \quad (27)$$

where w is a constant (See Propositions 16 and 23). The fact that the profile of the supercritical ring solutions is the well-known subcritical ground state profile, which is a well-behaved object, is a new and surprising phenomenon. This property is likely to lead to a considerable simplification in the analysis of the supercritical ring solutions. Indeed, the analysis of peak-type solutions in the critical case [17] was considerably easier for $d = 1$ than for $d \geq 2$, precisely because for $d = 1$ the ground state is given explicitly by the critical one dimensional sech profile.

Fig. 3 presents the classification of NLS singular ring solutions as a function of (σ, d) :

- (A) In the subcritical case ($\sigma d < 2$), all NLS solutions globally exist, hence no collapsing ring solutions exist.
- (B) The critical case $\sigma d = 2$ corresponds to $\alpha = 1$. In this case, the new asymptotic profile ψ_Q reduces to the ψ_G asymptotic profile (15). Since $r_m(t) = r_0 L(t)$, these solutions undergo *equal rate collapse*. The blowup rate of these critical ring solutions is a square root.
- (C) The supercritical case $2/d < \sigma < 2$ corresponds to $0 < \alpha < 1$. In this case, ring solutions collapse with the new asymptotic profile ψ_Q (21) at a $\frac{1}{1+\alpha}$ blowup rate. The

⁴ In this study we define the blowup rate as $L(t) = \frac{\|\psi(0, \cdot)\|_\infty^\sigma}{\|\psi(t, \cdot)\|_\infty^\sigma}$, see (6). Cazenave and Weissler define the blowup rate as $L(t) = \|\nabla \psi\|_2^{-1}$. These two definitions are equivalent (see Appendix A).

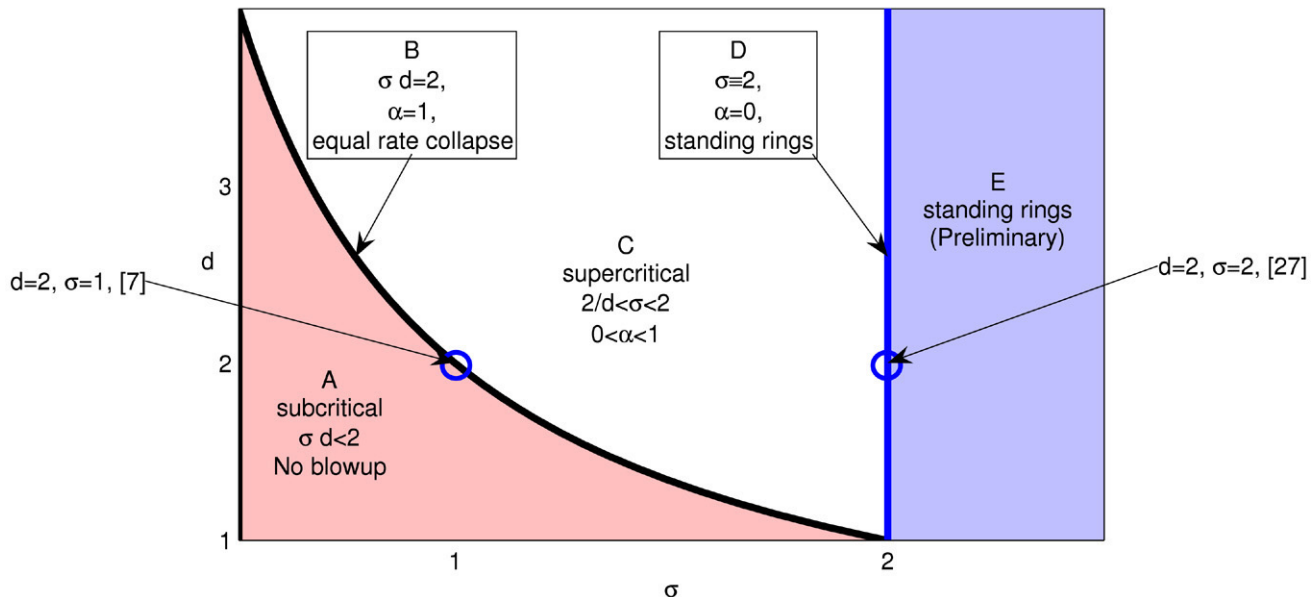


Fig. 3. Classification of singular ring solutions of the NLS as a function of σ and d .

ring radius decays to zero as $r_m(t) = r_0 L^\alpha(t)$, i.e. at a slower rate than $L(t)$.

- (D) The case $\sigma = 2$ corresponds to $\alpha = 0$. Since $r_m(t) \equiv r_0$, the solution is a collapsing standing ring. The blowup rate of these solutions is given by the loglog law (10).
- (E) Finally, in the case $\sigma > 2$ our preliminary numerical simulations suggest that it is characterized by standing ring solutions that collapse with a square root blowup rate with no loglog correction term, and with an asymptotic profile different from ψ_Q (Section 9).

1.4. Level of rigor

The derivation of the analytical results in this study (Propositions 1–3) is based on several assumptions and conjectures which have yet to be made rigorous. In particular, these results assume the existence of and convergence to the new asymptotic profile ψ_Q , see (21), and that the blowup rate is of the form $L(t) \sim (T_c - t)^p$ or slightly faster, see Conjecture 11. However, the impressive agreement between the analytical predictions of Propositions 1–3 and the numerical results (in particular, Figs. 23 and 24), provides a strong support to the validity of these assumptions.

At present, it is still an open problem whether the critical ring solution ψ_G is maintained all the way up to the singularity. In particular, this question arises since the profile G has an infinite L^2 norm. As we noted in [26], this does not necessarily conflict with the fact that the L^2 norm of the blowup solution is finite. The reason for this is that the collapsing solutions match the G profile only in the ring region, hence the slowly-decaying, infinite-power tail of the G profile may be “irrelevant” to the NLS solution.

There is no such infinite-power “problem” in the supercritical case, as the self-similar profile Q is given by a finite-power sech profile, see Eq. (27). Therefore, it is much more

likely that these ring solutions would indeed maintain the ring profile all the way up to the singularity.

1.5. Paper outline

The paper is organized as follows: in Section 2 we analyse ring solutions in the critical NLS and extend the results of [26] from $d = 2$ and $\sigma = 1$ to all $\sigma d = 2$ and $d > 1$. In Section 3 we present the first systematic numerical study of Raphael’s standing ring solutions. Section 4 is devoted to the analysis of singular ring solution for $2/d \leq \sigma \leq 2$ and $1 < d$. In particular, we derive the new asymptotic profile ψ_Q , see (21), relation (22) for the value of α , and the blowup rate of these singular rings solutions. In Section 5 we show that both critical and supercritical ring solutions undergo strong collapse. Section 6 is devoted to a systematic numerical study of the new singular ring solutions, which shows an excellent agreement between the numerical results and the analytic predictions of Section 4. In Section 7 we use a geometrical optics argument and numerical simulations to show that the ψ_Q profile is an attractor for high-power super-Gaussian initial conditions. In Section 8 we test numerically the stability of the new ring solutions and show that they are stable as solutions of the radially-symmetrical NLS, but unstable with respect to symmetry breaking perturbations. Finally, in Section 9 we present preliminary simulations of the case $\sigma > 2$. The numerical methods used in this study are described in Section 10.

2. Collapsing ring solutions of the critical NLS ($\sigma d = 2$)

In this section, we consider singular ring solutions of the critical NLS

$$i\psi_t(t, r) + \psi_{rr} + \frac{d-1}{r}\psi_r + |\psi|^{\frac{4}{d}}\psi = 0, \quad d > 1, \quad (28)$$

i.e. when $\sigma = 2/d$. In [26], we studied Eq. (28) when $d = 2$. We now extend these results to any $d > 1$.⁵

Proposition 4. Let ψ be a singular ring solution of the critical NLS (28) with an asymptotic self-similar blowup profile $\psi(t, r) \sim \psi_G(t, r)$ where

$$\psi_G(t, r) = \frac{1}{L^{d/2}(t)} G(\rho + r_0) e^{i\tau + i\frac{L}{4}r^2}, \quad \tau = \int_0^t \frac{ds}{L^2(s)},$$

$$\rho = \frac{r - r_m(t)}{L(t)}, \quad (29a)$$

and

$$r_m(t) = r_0 L(t), \quad (29b)$$

where G is a real-valued function and $r_0 = \arg \max G(r) > 0$. Then,

1. The blowup rate $L(t)$ is a square root, i.e.

$$\lim_{t \rightarrow T_c} \frac{L(t)}{\sqrt{T_c - t}} = \lim_{t \rightarrow T_c} \frac{\frac{d}{dt} L(t)}{\frac{d}{dt} (\sqrt{T_c - t})} = f_c > 0. \quad (30)$$

2. The self-similar ring profile $G(\rho)$ is the solution of

$$G''(\rho) + \frac{d-1}{\rho+r_0} G' + \left[\frac{f_c^4}{16} (\rho+r_0)^2 - 1 \right] G + G^{\frac{4}{d}+1} = 0, \quad -r_0 < \rho < \infty, \quad (31)$$

with the boundary conditions

$$G'(-r_0) = 0, \quad G(\infty) = 0.$$

Proof. The blowup rate of the critical NLS has the rigorous bound $L(t) \leq M\sqrt{T_c - t}$, where M is a constant [32,33]. Therefore, we only need to consider the case where the blowup rate is equal to or faster than a square root. In Proposition 1 in [26], we showed that if the blowup rate is a square root then G is a solution of (31). In Proposition 3 in [26], we showed that if the blowup rate is faster than a square root then G is the solution of (5).⁶ Since Eq. (5) does not admit ring solutions (see Appendix C), it follows that the blowup rate is a square root and that G is a solution of (31). \square

Proposition 4 describes singular solutions of the NLS that have the following characteristics:

- (1) The collapsing part of the solution has a self-similar ring profile G .
- (2) The blowup rate L is a square root.
- (3) Equal-rate collapse, i.e. the ring width $L(t)$ and radius $r_m(t)$ go to zero at the same rate, see Eq. (29b).

Since in [26] we considered only the case $d = 2$, we now present numerical results for $d \neq 2$. For example, in Fig. 4

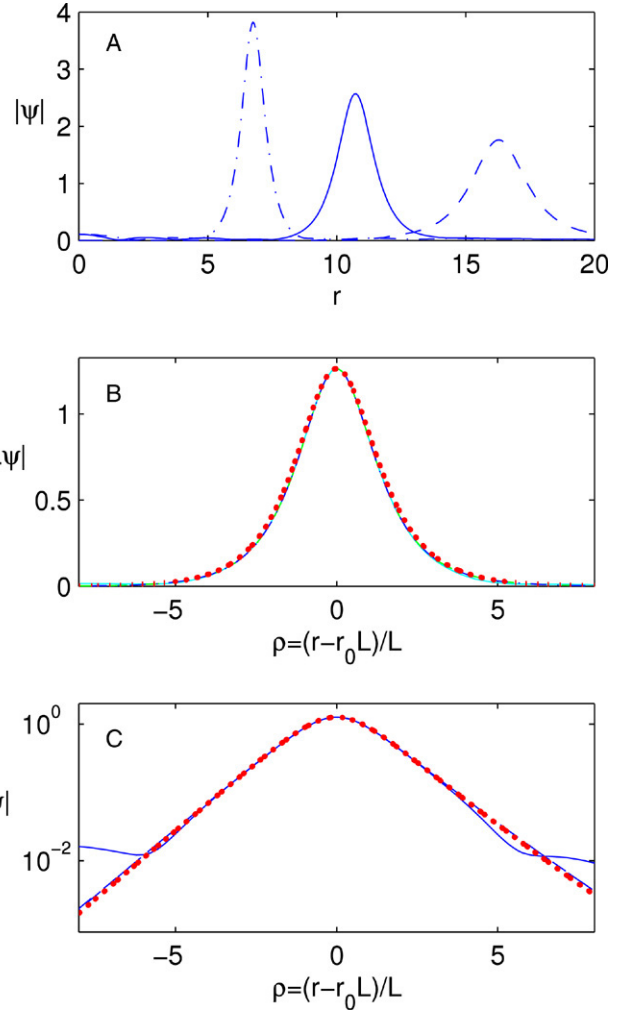


Fig. 4. A: Solution of the critical NLS (28) with $d = 7/4$ and with the initial condition ψ_G^0 at $t = 1.04$ ($1/L = 1.01$, dashes), $t = 5.73$ ($1/L = 1.61$, solid) and $t = 7.89$ ($1/L = 2.45$, dash-dots). B: The solution at focusing levels $1/L = 1.61$ (solid), $1/L = 3.20 \times 10^8$ (dashes) and $1/L = 2.90 \times 10^{13}$ (dash-dots), normalized according to (33). Dotted curve is the G profile with $r_0 \approx 16.8392$, $G(-r_0) \approx 3.373 \times 10^{-5}$ and $f_c \approx 0.3705$. All four curves are indistinguishable. C: Same data as in B on a semilogarithmic scale.

we solve the critical NLS (28) for $d = 7/4$ with the G -profile initial condition

$$\psi_G^0 = G(r + r_0) e^{-i\frac{f_c^2}{8}r^2}, \quad (32)$$

where $G(r)$ is the solution of the Eq. (31) with $G(-r_0) = 5 \times 10^{-5}$, and $f_c \approx 0.376$. Fig. 4A shows that the numerical solution indeed collapses with a ring profile. In order to check for self-similarity, in Fig. 4B we rescale the numerical solution according to⁷

$$\psi_{\text{rescaled}} = \frac{1}{L^{1/\sigma}(t)} \psi \left(\frac{r - r_m(t)}{L} \right),$$

$$L(t) = \frac{\max_r |\psi|^\sigma}{\max_r |\psi|^\sigma}, \quad r_m(t) = r_m(0)L(t), \quad (33)$$

⁵ The definition of ρ in Proposition 4 is different from its definition in [26], in order to conform to the notations used in this paper where $\rho = 0$ is the location of the ring peak.

⁶ Although Propositions 1 and 2 in [26] were proved for $d = 2$, the proof for the general case ($d \neq 2$) is identical.

⁷ Note that under the normalization (33), $\max_r |\psi_{\text{rescaled}}| = \max_r |\psi_0|$.

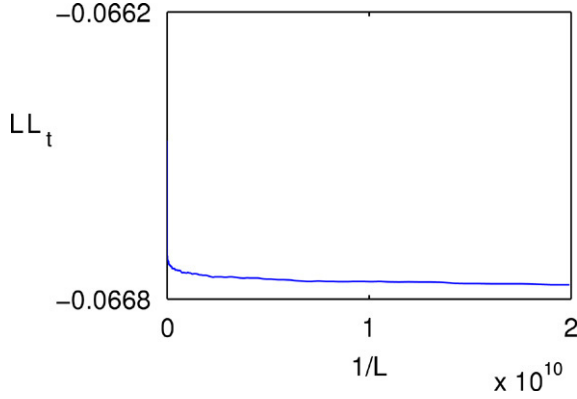


Fig. 5. Determining the blowup rate of the solution of Fig. 4.

where $r_m(0) = 16.83$ and $\sigma = 2/d$. As expected, the normalized solution remains unchanged while focusing by a factor of 10^{10} , indicating that the solution indeed undergoes self-similar collapse. In addition, the self-similar profile is in excellent match with G , which is the solution of Eq. (31) with $r_0 \approx 16.8392$, $G(-r_0) \approx 3.373 \times 10^{-5}$ and $f_c \approx 0.3705$. A closer look on the same data on a semilogarithmic scale (Fig. 4C) shows that the solution is “only” quasi self-similar. Indeed, the self-similar profile ψ_G characterizes only the collapsing ring region but not the inner and outer regions, i.e.

$$\psi(t, r) \sim \begin{cases} \psi_{\text{inner}} & 0 \leq r < \rho_1 L(t) \\ \psi_G & \rho_1 L(t) \leq r \leq \rho_2 L(t) \\ \psi_{\text{outer}} & \rho_2 L(t) < r, \end{cases} \quad (34)$$

where $1 \ll \rho_1 \ll r_0 \ll \rho_2$.

We now consider the blowup rate of the solution of Fig. 4. In general, it is hard to distinguish a strictly square root blowup rate from a square root blowup with a small (e.g. *loglog*) correction. In order to do that, we monitor the dynamics of $LL_t = \frac{1}{2}(L^2)_t$ (see Section 10.2 for details on how LL_t is recovered from the simulation), since $\lim_{t \rightarrow T_c} LL_t = -f_c^2/2 < 0$ in the case of a strict square root blowup rate

$L(t) \sim f_c \sqrt{T_c - t}$, whereas $\lim_{t \rightarrow T_c} LL_t = 0$ when the blowup rate is faster than a square root [26]. Indeed, in Fig. 5 we see that $\lim_{t \rightarrow T_c} LL_t = -0.06667 = -\frac{f_c^2}{2} < 0$, indicating that $L \sim 0.365 \sqrt{T_c - t}$, i.e. that the blowup rate is a square root.

Finally, we consider the stability of ψ_G . To do so, we randomly perturb the initial ring profile from Fig. 4 as

$$\psi_G^{0, \text{noise}} = (1 + \varepsilon_1(r))\psi_G^0 + \varepsilon_2(r), \quad (35)$$

where $\varepsilon_1(r)$ and $\varepsilon_2(r)$ are uniformly distributed in $[-0.3, 0.3]$ and in $[-0.1, 0.1]$, respectively. After focusing by a factor of ≈ 1.09 , the noise in the ring region (i.e. the area of high nonlinearity) disappears (Fig. 4B). Subsequently, the noise at the inner and outer regions also decreases, until after focusing by a factor of ≈ 10 , the solution approaches a clean asymptotic ring profile ψ_G (Fig. 4C). Therefore, we conclude that ψ_G is a strong attractor.

In [26], it was shown numerically for the two-dimensional critical case ($d = 2$, $\sigma = 1$) that ψ_G is stable as a solution of Eq. (28) under radial perturbations such as (35), but unstable as a solution of

$$i\psi_t(t, x, y) + \Delta\psi + |\psi|^2\psi = 0, \quad \Delta = \partial_{xx} + \partial_{yy}, \quad (36)$$

with respect to perturbations that breakup the radial symmetry. When $d = 7/4$, the radially-symmetrical NLS (28) has no analogue such as (36), therefore there is no notion of stability with respect to symmetry-breaking perturbations in this case.

3. Raphael’s standing ring solutions of the supercritical NLS ($d = 2$, $\sigma = 2$)

3.1. Theory

Consider the quintic two-dimensional radially-symmetrical NLS

$$i\psi_t(t, r) + \psi_{rr} + \frac{1}{r}\psi_r + |\psi|^4\psi = 0, \quad \psi(0, r) = \psi_0(r). \quad (37)$$

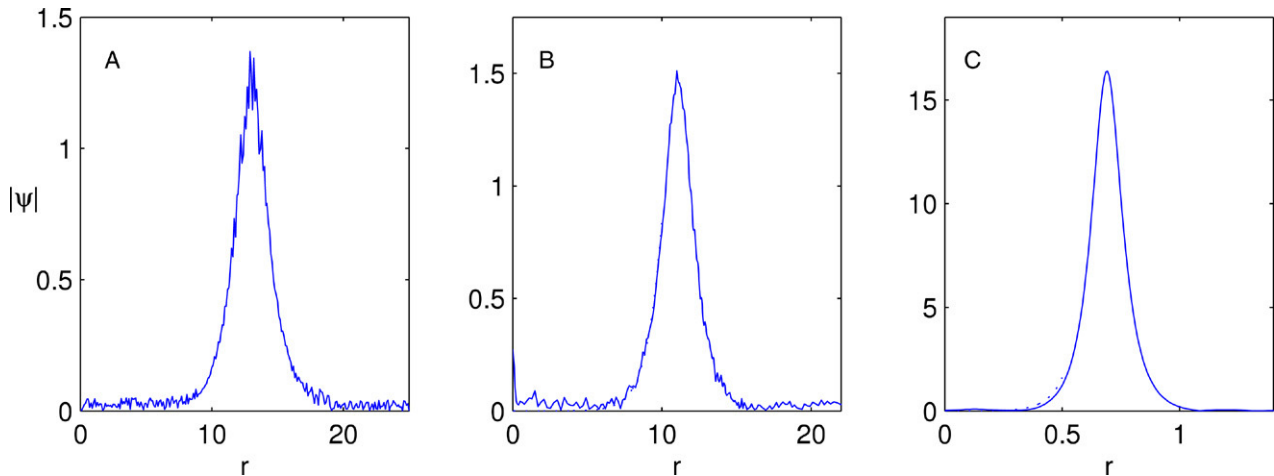


Fig. 6. Solution of the critical NLS (28) with $d = 1.75$ and the noisy initial condition (35) at A: $t = 0$ ($1/L = 1$); B: $t = 1.96$ ($1/L = 1.09$); C: $t = 6.98$ ($1/L = 10.03$). Dotted curve in B and C is the asymptotic ψ_G profile (29), the two curves are nearly indistinguishable.

This equation is supercritical, since $\sigma d = 2 \cdot 2 > 2$. As noted in Section 1, until recently, the only known stable singular solutions of supercritical NLS equations had a self-similar peak profile, i.e. $\psi(t, r) \sim \psi_S(t, r)$, where

$$\psi_S(t, r) = \frac{1}{L^{1/\sigma(t)}} S(\rho) e^{i\tau + i\frac{L_t}{4L} r^2},$$

$$\tau = \int_0^t \frac{ds}{L^2(s)}, \quad \rho = \frac{r}{L(t)}, \quad (38)$$

and S is the “peak-type” solution of

$$S_{\rho\rho} + \frac{d-1}{\rho} S_\rho + \left(\frac{f_c^2}{16} \rho^2 - 1 - i \frac{f_c(\sigma d - 2)}{4} \right) S$$

$$+ |S|^{2\sigma} S = 0, \quad (39)$$

$$S'(0) = 0, \quad S(\infty) = 0.$$

In addition, these solutions have a square-root blowup rate, i.e. $L(t) \sim f_c \sqrt{T_c - t}$.

Recently, Raphael proved the existence and stability of a new type of singular solutions of Eq. (37) that have a self-similar ring profile:

Theorem 5 ([27]). *Let*

$$P = \sqrt[4]{3} \sqrt{\operatorname{sech}(2r)} \quad (40)$$

be the solution of

$$P''(r) - P + P^5 = 0, \quad P'(0) = 0, \quad P(\infty) = 0. \quad (41)$$

There exists an open subset $H \subset H_r^1$ such that the following holds:

Let $\psi_0 \in H$, then the corresponding solution ψ to (37) blows up in finite time $0 < T_c < \infty$ according to the following dynamics:

- (1) *Description of the singularity formation: there exist $L(t) > 0$, $r_m(t) > 0$ and $\tau(t) \in \mathbb{R}$ such that*

$$\psi(t, r) - \psi_P(t, r) \xrightarrow{L^2} \psi_{bg}(r) \quad \text{as } t \rightarrow T_c, \quad (42)$$

where

$$\psi_P = \frac{1}{\sqrt{L(t)}} P(\rho) e^{i\tau(t)}, \quad \rho = \frac{r - r_m(t)}{L(t)}, \quad (43)$$

such that the radius of the singular circle converges to a positive constant, i.e.

$$\lim_{t \rightarrow T_c} r_m(t) = r_m(T_c) > 0.$$

- (2) *Estimate on the blowup rate:*

$$\lim_{T_c - t} L(t) \left(\frac{\log |\log(T_c - t)|}{T_c - t} \right)^{\frac{1}{2}} = \frac{\sqrt{2\pi}}{\|P\|_{L^2}}. \quad (44)$$

Theorem 5 proves the existence of singular ring solutions of the quintic two-dimensional NLS (37) that have the following properties:

1. The collapsing part of the solution, ψ_P has a self-similar ring profile.

2. The blowup rate is a square root with a loglog correction.
3. The ring is *standing*, i.e. the ring’s radius $r_m(t)$ approaches a positive constant as the solution collapses.

Raphael’s solutions are different from all previously known singular solutions of the NLS, since they blow up on the circle $r = r_m(T_c) > 0$, whereas all other known singular solutions of the NLS collapse at a point.

3.2. Motivation for Theorem 5

The motivation for **Theorem 5** is as follows: for a standing ring solution ψ_P , $\psi_{rr} \sim \frac{1}{L^2(t)}$ and $\frac{1}{r} \psi_r \sim \frac{1}{r_m(T_c)} \frac{1}{L(t)}$ in the ring region. Therefore, as $t \rightarrow T_c$, the $\frac{1}{r} \psi_r$ term in Eq. (37) becomes negligible compared with ψ_{rr} in the ring region $r \approx r_m(T_c)$. Hence, near the singularity, Eq. (37) reduces to the one-dimensional critical NLS

$$i\psi_t(t, r) + \psi_{rr} + |\psi|^4 \psi = 0. \quad (45)$$

From NLS theory [17,34] it follows that for solutions of Eq. (45) whose peak at time t is at $r_m(t)$, the collapsing core blows up with the self-similar P profile (40) at the loglog law blowup rate, i.e.

$$\psi_P = \frac{1}{\sqrt{L(t)}} P \left(\frac{r - r_m(t)}{L} \right) e^{i\tau(t) + i\frac{L_t}{4L} (r - r_m(t))^2}, \quad (46)$$

where L satisfies (44). Therefore, we “recover” the results of **Theorem 5** on the asymptotic profile (43) (but see Section 3.2.1) and on the blowup rate.

Remark 6. In fact, since collapse in the critical NLS is highly sensitive to small perturbations [1], the validity of using (45) to approximate (37) is not obvious. Indeed, while this approximation will prove useful for $\sigma = 2$ and any $d > 1$ (see Section 4.2), it will fail for $\sigma < 2$ (see Section 4.4).

3.2.1. Radial phase

According to **Theorem 5**, the asymptotic profile of the collapsing part of the solution is given by

$$\psi_P = \frac{1}{\sqrt{L}} P \left(\frac{r - r_m(t)}{L} \right) e^{i\tau(t)}.$$

However, from the analysis in [27] and by (46), this asymptotic profile also has a radial dependence in the phase:

Lemma 7. *The asymptotic profile ψ_P of the collapsing part of standing ring solutions of Eq. (37) is given by*

$$\psi_P = \frac{1}{\sqrt{L}} P(\rho) e^{i\tau(t) + iS(t, \rho)}, \quad \rho = \frac{r - r_m(t)}{L},$$

$$\tau(t) = \int_0^t \frac{ds}{L^2(s)}, \quad (47a)$$

where

$$S = \frac{L_t}{4L} (r - r_m(t))^2. \quad (47b)$$

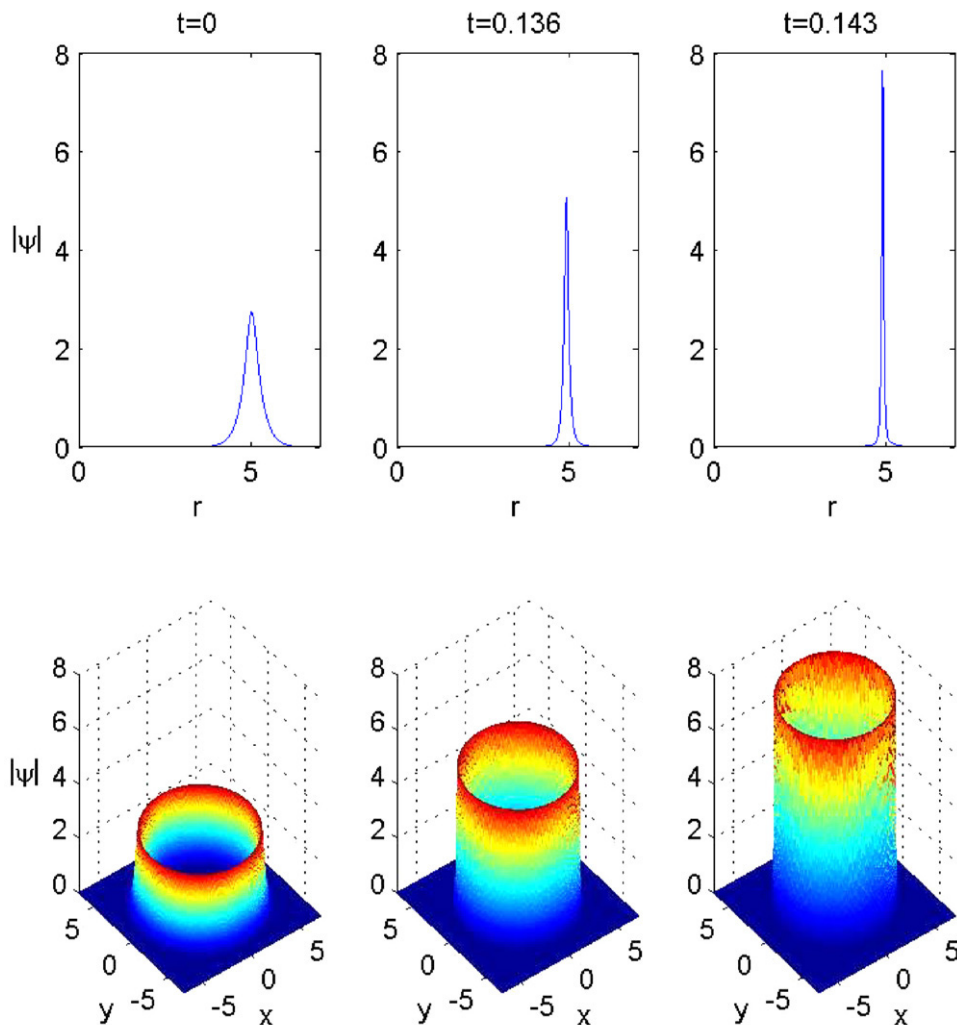


Fig. 7. Solution of the quintic NLS (37) with ψ_0 given by (49).

The phase S does not appear in Eq. (43), since it decays to zero at the singularity. Indeed, since $\rho = \frac{r-r_m(t)}{L}$, then $S = \frac{LL_t}{4}\rho^2$. According to Theorem 5, L is given by the loglog law, hence $LL_t \rightarrow 0$. Since $\rho = \mathcal{O}(1)$ in the ring region, we see that $\lim_{\substack{t \rightarrow T_c \\ \rho = \mathcal{O}(1)}} S = 0$. As we shall see in Section 4, this radial phase will be vital for our analysis of the supercritical ring solutions.

3.3. Numerical study

It is remarkable that Raphael discovered and proved the existence and stability of the standing ring solutions without any numerical simulations. We now present a systematic numerical study of Raphael's standing ring solutions. The goals of these simulations are

- (1) To present the first numerical observation of Raphael's standing ring solutions.
- (2) To test the stability of the standing ring solutions. According to Theorem 5, these solutions are stable with respect to radially-symmetrical perturbations. However,

Theorem 5 does not give an indication to the size of the basin of attraction of these solutions.

- (3) To test the stability of the standing ring solutions with respect to symmetry-breaking perturbations, i.e. as solutions of the supercritical quintic two-dimensional NLS

$$i\psi_t(t, x, y) + \Delta\psi + |\psi|^4\psi = 0, \quad \Delta = \partial_{xx} + \partial_{yy}. \quad (48)$$
- (4) To confirm that the radial phase of the standing ring solutions is given by (47b).
- (5) To serve as a benchmark for the numerical investigation of ring solutions in the general supercritical NLS in Section 6, where analytical results on the blowup rate are unavailable.

3.3.1. Blowup profile

We solve the quintic two-dimensional radially-symmetric NLS (37) with the initial condition

$$\psi_p^0 = P(r-5) = \sqrt[4]{3}\sqrt{\operatorname{sech}(2(r-5))}. \quad (49)$$

In Fig. 7, we plot the early stages of the collapse as the solution focuses by a factor of ≈ 3 . As predicted by Theorem 5, as the ring amplitude increases and the ring width shrinks, the ring

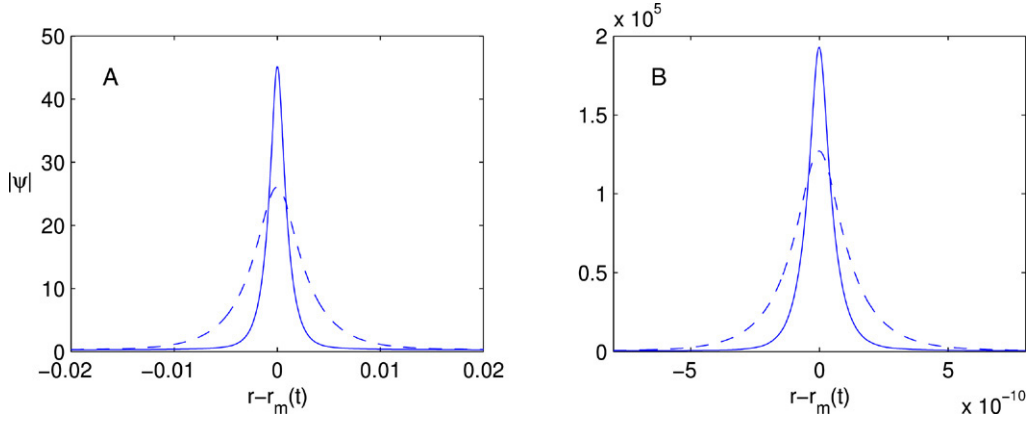


Fig. 8. Solution of Fig. 7 at A: $t = 0.144197$ ($L^{-1} = 390.2$, $r_m(t) = 4.87745$, dashes), $t = 0.1442062$ ($L^{-1} = 1174.3$, $r_m(t) = 4.87739$, solid), B: $L^{-1} = 9.29 \times 10^9$ ($r_m(t) = 4.87737$, dashes), $L^{-1} = 2.14 \times 10^{10}$ ($r_m(t) = 4.87737$, solid). Values of t in graph B differ only in the 14th digit or after, therefore only the focusing levels $1/L$ are quoted.

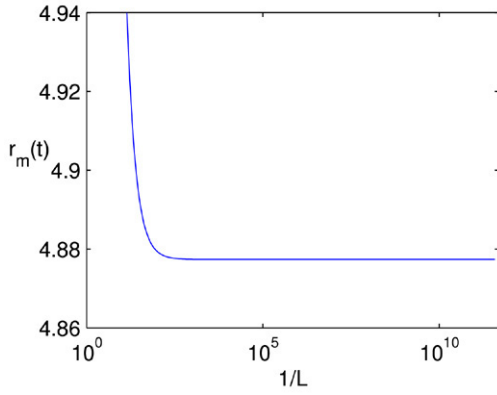


Fig. 9. Ring radius $r_m(t)$ as a function of the focusing factor $1/L$ for the solution of Fig. 7.

radius does not go to zero, but rather converges to a positive constant. In Fig. 8, we plot the solution as it continues to collapse over 10 orders of magnitude. As in Fig. 7, the ring amplitude grows larger and larger and its width narrower and narrower, while the ring radius $r_m(t)$ hardly changes. In Fig. 9 we plot $r_m(t)$ as a function of the focusing factor $1/L$. It can be seen that $\lim_{t \rightarrow T_c} r_m(t) \cong 4.8773$, i.e. the ring is standing and not shrinking towards the origin.

To confirm that the collapse is indeed self-similar, i.e. of the form

$$|\psi| \sim \frac{1}{L^{1/\sigma(t)}} P\left(\frac{r - r_m(t)}{L(t)}\right) \quad (50)$$

with $\sigma = 2$, we rescale the solution ψ according to

$$\psi_{\text{rescaled}} = L^{1/\sigma} \psi\left(\frac{r - r_m(t)}{L}\right), \quad L = \frac{\max_r |\psi_0|^\sigma}{\max_r |\psi|^\sigma}, \quad (51)$$

$$r_m(t) = \operatorname{argmax}_r |\psi|.$$

The only difference between the rescalings (33) and (51) is in the calculation of $r_m(t)$. In (33), the dependence of the ring radius $r_m(t)$ on $L(t)$ is analytically known and therefore can be

used in the rescaling. However, in the case of supercritical rings the relation between $r_m(t)$ and $L(t)$ is not known, therefore it is recovered from the solution. Fig. 10 shows that all rescaled plots of the solution at focusing levels varying from $L^{-1} = 10^1$ to $L^{-1} = 10^{10}$ are indistinguishable, indicating that the solution is indeed self-similar while focusing over 10 orders of magnitude. The rescaled profiles are in perfect fit with the P profile (40) around the peak $r = r_m(t)$. Plotting the same data on a semi-logarithmic scale (Fig. 10B) shows that the rescaled profile is self-similar around the peak $r \approx r_m(t)$, or more precisely, for $\rho = (r - r_m(t))/L = \mathcal{O}(1)$, but not near the beam centre ($\rho \ll -1$) or far outside ($\rho \gg 1$), in agreement with the analysis in [27]. Hence, as in the case of the critical G profile ring solution (see Section 2), Raphael's standing ring solutions are “only” quasi self-similar.

To observe the radial phase (47b), we show in Fig. 11 that in the ring region $-5 \leq \rho \leq 5$ the phase of the numerical solution $S_{\text{numerical}}$ is nearly indistinguishable from the phase $S_{\text{predicted}}$ predicted in (47b). To calculate $S_{\text{predicted}}$, we recover LL_t from the numerical solution (see Section 10.2 for more details) and calculate

$$S_{\text{predicted}}(\rho) = S_{\text{predicted}}(0) + \frac{LL_t}{4} \rho^2,$$

where $S_{\text{predicted}}(0) = S_{\text{numerical}}(0)$.

3.3.2. Blowup rate

Next, we consider the blowup rate of the standing ring solutions. To do so, we first assume that $L \sim f_c(T_c - t)^p$ and find the best fitting p (see Section 10.2 for details on how L is recovered from the simulation). Fig. 12A shows that $p \approx 0.5001$, indicating that the blowup rate is square root or slightly faster. Next, we check whether L is slightly faster than a square root, by plotting LL_t as a function of the focusing factor $1/L$. Recall that for a square root blowup rate, LL_t will go to a negative constant as $t \rightarrow T_c$, while for a faster-than-a-square root blowup rate LL_t goes to zero [26]. The graph of Fig. 12B does not give a conclusive evidence as to whether LL_t goes to a negative constant or to zero. However, we know

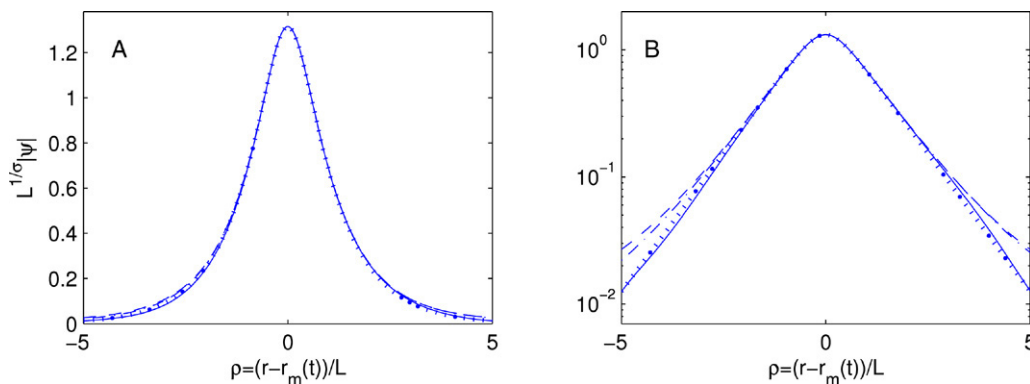


Fig. 10. A: Solution of Fig. 8 rescaled according to Eq. (51) at $t = 0.05$ ($1/L = 5$, solid), $t = 0.14420739600$ ($1/L = 3.58 \times 10^5$, dashes), and $t = 0.14420739601$ ($1/L = 1.35 \times 10^{10}$, dot-dashes). Dotted curve is $P = \sqrt[4]{3} \sqrt{\text{sech}(2\rho)}$. All four curves are indistinguishable around the peak $r = r_m(t)$. B: Same data on a semi-logarithmic scale.

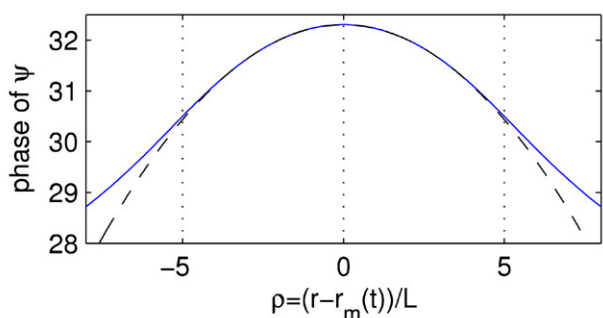


Fig. 11. Phase $S_{\text{numerical}}$ of the solution of Fig. 8 at $L^{-1} = 6.31 \times 10^5$ (solid). Dashed curve is $S_{\text{predicted}} = \tau + \frac{LL_t}{4} \rho^2 = 32.3 - 0.07467 \rho^2$. The two curves are indistinguishable for $-5 \leq \rho \leq 5$.

from Theorem 5 that the blowup rate is given by the loglog law. Therefore, Fig. 12B provides an example of a “typical” plot of a faster than a square root blowup rate. In contrast, Fig. 5 provides an example in which LL_t goes to a negative constant and the blowup rate is a square root. Since these two graphs are “sufficiently different” from each other, in the subsequent sections we will use Figs. 5 and 12B as “benchmarks” for

determining the blowup rate in cases where analytical results on the blowup rate are unavailable.

3.3.3. Stability

In order to test the radial stability of Raphael’s standing ring solutions, we randomly perturb the initial ring profile from Fig. 8 as follows:

$$\psi_p^{0,\text{noise}} = (1 + \varepsilon_1(r))\psi_p^0 + \varepsilon_2(r), \quad (52)$$

where $\varepsilon_1(r)$ and $\varepsilon_2(r)$ are uniformly distributed in $[-0.3, 0.3]$ and in $[-0.1, 0.1]$, respectively. Note that for this initial condition both the ring and the inner and outer regions are perturbed (see Fig. 13A). After focusing by a factor of ≈ 1.2 , the noise in the ring region (i.e. the area of high nonlinearity) disappears (Fig. 13B). Subsequently, the noise at the inner and outer regions also decreases, until after focusing by a factor of ≈ 6 , the solution approaches a clean standing ring profile (Fig. 13C). We, therefore, conclude that the standing ring solutions ψ_Q , see Eq. (47), are strong attractors in the radially-symmetrical case. Of course, we know from Theorem 5 that the standing ring solutions are stable with respect to radially-symmetrical perturbation. However, Theorem 5 does not give an indication as to the magnitude of

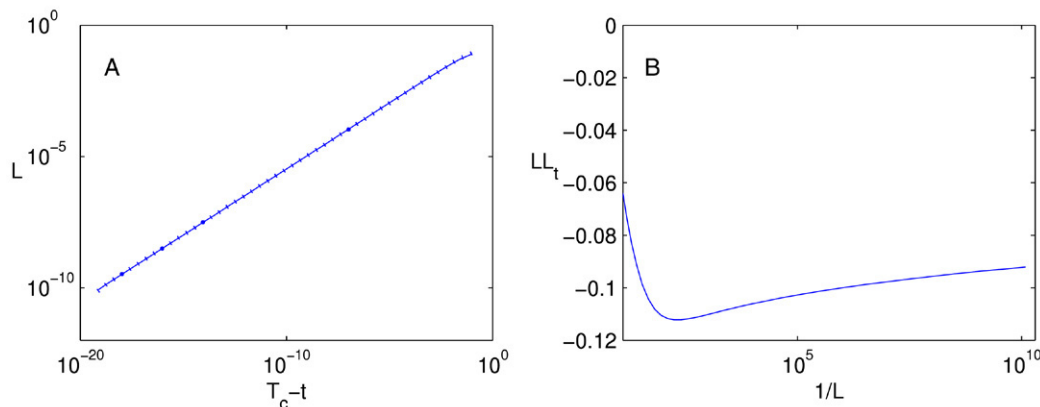


Fig. 12. A: L as a function of $T_c - t$ (solid) for the solution of Fig. 8. Dotted curve is the fitted curve $c(T_c - t)^{0.5001}$ where $c = 0.341$. B: LL_t as a function of the focusing factor $1/L$.

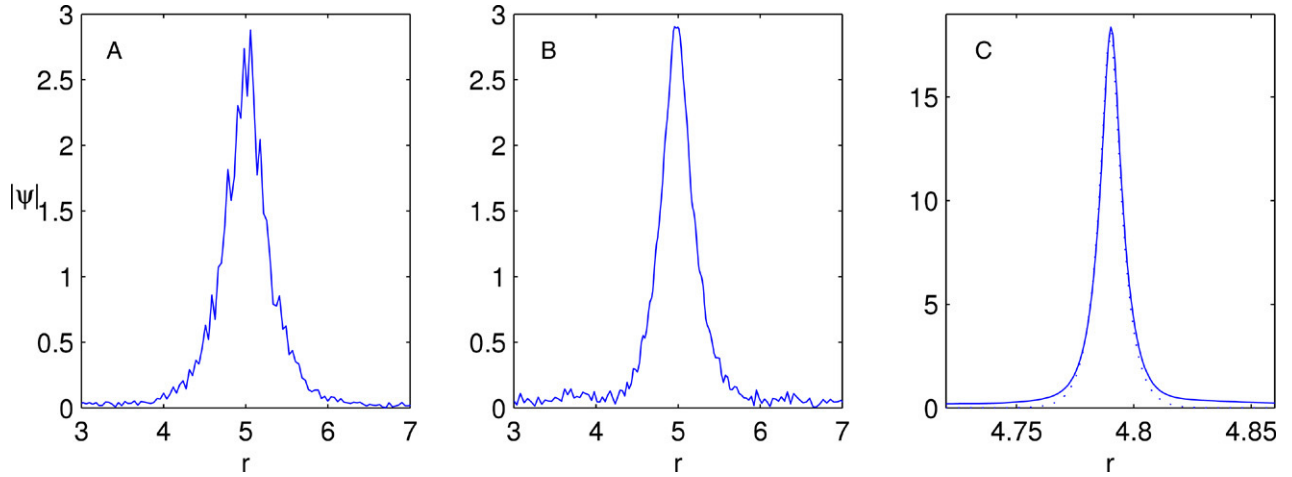


Fig. 13. Solution of the quintic 2D NLS (37) with the (slightly focused) noisy initial condition (52). A: $t = 0$, $1/L = 1.5$. B: $t = 0.0661$, $1/L = 1.677$. C: $t = 0.195$, $1/L = 10.61$ (solid). Dotted curve is the modulated P profile (40).

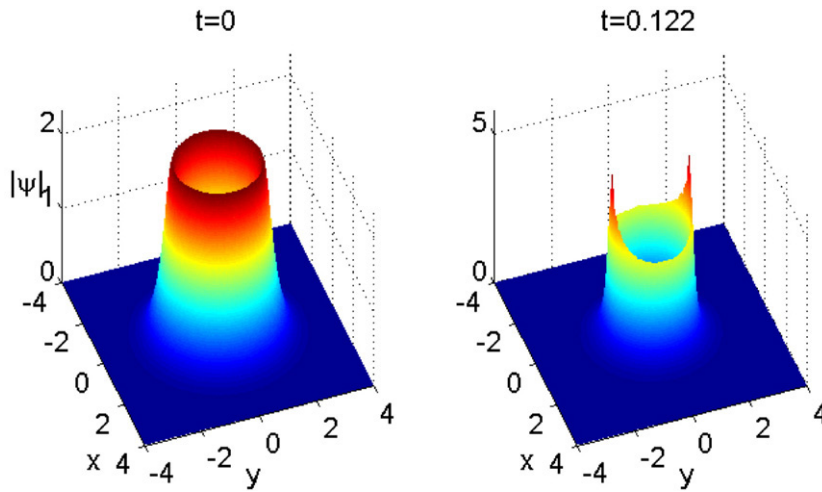


Fig. 14. Solution of the NLS (48) with slightly elliptical initial condition (53).

their basin of attraction. This numerical example, as well as other tests that we conducted, show that the basin of attraction of these solutions is of significant magnitude.

In [27], Raphael did not consider the stability of standing ring solutions with respect to anisotropic perturbations. We now test the stability of the standing ring solutions as solutions of the NLS (48). To do that, we deterministically breakup the symmetry of the initial-condition (49) by inducing a small ellipticity to the initial condition, i.e.

$$\psi_P^{0,\text{elliptic}} = \psi_P^0(\sqrt{1.02x^2 + y^2}). \tag{53}$$

After very little focusing (≈ 1.5), the ring breaks into two filaments that are located on the intersection of the ring with the x -axis (see Fig. 14 and also Section 10.3). Therefore, we conclude that Raphael’s standing ring solutions are highly unstable with respect to perturbations that break up the radial symmetry. This result is not surprising, since in numerous studies it has been found that a ring is an unstable structure in the NLS (see e.g. [35–37,26,38–40]).

4. Analysis of supercritical ring solutions

All the NLS singular ring solutions observed until now (see Sections 2 and 3) have been of the form

$$|\psi| \sim \frac{1}{L^{1/\sigma}(t)} F\left(\frac{r - r_m(t)}{L(t)}\right).$$

These solutions have the following characteristics:

1. The rings amplitude scales as $L^{-1/\sigma}$ and blows up as its width L goes to zero.
2. The ring radius $r_m(t)$ converges either to zero or to a positive constant as $t \rightarrow T_c$. In the first case, blowup occurs at the origin. In the latter case, the solution blows up on a d -dimensional sphere.

In Section 2, we presented ring solutions of the critical NLS ($\sigma d = 2$) that undergo *equal-rate collapse*, i.e., $r_m(t) = r_0 L(t)$. In Section 3, we presented standing ring solutions of the quintic two-dimensional NLS ($d = 2, \sigma = 2$) that collapse

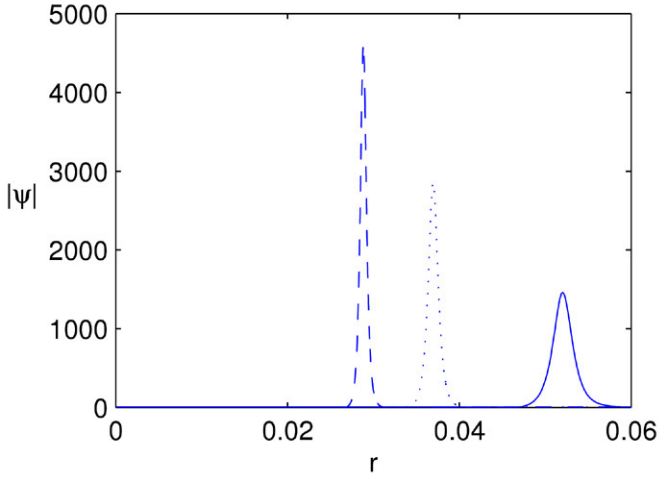


Fig. 15. Solution of the supercritical NLS (54) with initial condition $\psi_0 = 10e^{-r^4}$ at $t = 0.038711$ (solid), $t = 0.038720$ (dots) and $t = 0.038723$ (dashes).

in amplitude and width, but the ring radius does not go to zero, i.e. $r_m(t) \rightarrow r_m(T_c) > 0$.

We now ask, *do singular ring solutions exist in other cases and if so, how do they behave?* For example, in [26], we presented preliminary simulations of the supercritical three-dimensional cubic NLS ($d = 3, \sigma = 1$)

$$i\psi_t(t, r) + \psi_{rr} + \frac{2}{r}\psi_r + |\psi|^2\psi = 0. \quad (54)$$

We showed that, as in the critical case, there exist solutions that collapse with a ring profile (see Fig. 15). However, unlike the critical case, the ring radius of these solutions decayed to zero as $r_m(t) \approx cL^p(t)$ where $p \approx 0.49993$, i.e. at a slower rate than the ring width L . These collapsing solutions are also not standing ring solutions, since the ring radius shrinks to zero as the solution approaches the singularity, $\lim_{t \rightarrow T_c} r_m(t) = 0$.

We now analyse collapsing ring solutions of the radially-symmetrical supercritical NLS equation

$$i\psi_t(t, r) + \psi_{rr} + \frac{d-1}{r}\psi_r + |\psi|^{2\sigma}\psi = 0, \quad (55)$$

$$2/d \leq \sigma \leq 2, 1 < d.$$

We do not consider the case of $d = 1$, since in one dimension there is no meaning to a ring solution, as $r = 0$ is no different than $r > 0$. In addition, we consider only the case $\sigma d \geq 2$, since this is a necessary condition for collapse.

The asymptotic profile that has been used in the asymptotic analysis of *all* singular solutions of the NLS (both peak-type and ring-type) is

$$\psi_F = \frac{1}{L^{1/\sigma}} F\left(\frac{r}{L}\right) e^{i\tau + i\frac{L}{4L}r^2}, \quad \tau = \int_0^t \frac{ds}{L^2(s)}, \quad (56)$$

see (6). For a ring profile with radius r_0 , it is convenient to define $G(r) = F(r + r_0)$, so that in terms of G , the peak of the ring is at $\rho = 0$. This shift gives rise to the asymptotic

profile

$$\psi_G = \frac{1}{L^{1/\sigma}} G\left(\frac{r - r_m(t)}{L}\right) e^{i\tau + i\frac{L}{4L}r^2},$$

$$\tau = \int_0^t \frac{ds}{L^2(s)}, \quad (57a)$$

where

$$r_m(t) = r_0 L(t), \quad (57b)$$

see Eq. (29). The asymptotic profile (57) describes ring solutions that undergo *equal-rate collapse*, see (57b). In this case, $\lim_{t \rightarrow T_c} r_m(t) = 0$, i.e. the ring radius shrinks to zero.

The asymptotic form of Raphael's standing ring solutions, as given by Theorem 5 together with our addition of the quadric phase term (47b), is

$$\psi_P = \frac{1}{L^{1/\sigma}} P\left(\frac{r - r_m(t)}{L}\right) e^{i\tau + i\frac{L}{4L}(r - r_m(t))^2},$$

$$\tau = \int_0^z \frac{ds}{L^2(s)}, \quad (58a)$$

where

$$\lim_{t \rightarrow T_c} r_m(t) = r_m(T_c) > 0, \quad (58b)$$

see Eq. (46). This form is similar to the asymptotic form (57), but with two important differences:

1. The quadratic phase term is centred at $r = 0$ in (57), corresponding to focusing towards the origin, but at $r = r_m(t)$ in (46), corresponding to focusing towards $r_m(t)$.
2. The ring radius $r_m(t)$ is $r_m(t) = r_0 L(t)$ in (56) but $r_m(t) \equiv r_0$ in (58).

We now ask: *What is the asymptotic profile ψ_Q and blowup rate of ring solutions such as in Fig. 15?* Let us note that the ring radius is $r_m(t) = r_0 L(t)$ in ψ_G , $r_m(t) = r_0$ in ψ_P and $r_m(t) \approx r_0 \sqrt{L(t)}$ for the ring solutions ψ_Q as in Fig. 15. Therefore, the blowup profile ψ_Q of these solutions is different from ψ_G and ψ_P , but appears to be “somewhere between” these two asymptotic profiles. Therefore, we construct the asymptotic profile ψ_Q by “interpolating” ψ_G and ψ_P .

First we “interpolate” the “common components” of ψ_G and ψ_P . In both ψ_G and ψ_P , the solution ψ is self-similar around the ring radius $r_m(t)$, i.e.

$$|\psi| \sim \frac{1}{L^{1/\sigma}} Q(\rho), \quad \rho = \frac{r - r_m(t)}{L},$$

see (57) and (58). Therefore, we will retain this form in the new asymptotic profile. Next, we “interpolate” the “different components” of the two asymptotic profiles ψ_G and ψ_P as follows:

- (1) We linearly interpolate the two quadratic phase terms of (57) and (58), so that they describe ring solutions whose radius shrinks to zero, but at the same time their width shrinks toward $r_m(t)$.
- (2) We set $r_m(t) = r_0 L^\alpha$, so that (57b) and (58b) correspond to $\alpha = 1$, and $\alpha = 0$, respectively, and the new ring solutions correspond to $0 < \alpha < 1$.

Therefore, our starting point is the asymptotic profile

$$\psi_Q = \frac{1}{L^{1/\sigma}} Q \left(\frac{r - r_0 L^\alpha}{L} \right) e^{i\tau + i\gamma(t)r^2 + i\delta(t)(r - r_0 L^\alpha)^2}. \quad (59)$$

Substitution of the form (59) into the supercritical NLS (55) gives

$$Q_{\rho\rho} + (d-1) \frac{L}{L\rho + r_0 L^\alpha} Q_\rho - Q + Q^{2\sigma+1} - A Q + i(B + \rho C) Q_\rho + iD Q = 0, \quad (60)$$

where

$$A = (L\rho + r_0 L^\alpha)^2 L^2 \gamma_t(t) + L^4 \rho^2 \delta_t(t) - 2\alpha \rho r_0 L^{2+\alpha} L_t \delta(t) + 4L^2 (\gamma(t)(L\rho + r_0 L^\alpha) + \delta(t)L\rho)^2,$$

$$B = -r_0 \alpha L^\alpha L_t + 4\gamma(t)r_0 L^{\alpha+1},$$

$$C = -LL_t + 4(\gamma(t) + \delta(t))L^2,$$

$$D = -\frac{1}{\sigma} LL_t + 2[d \cdot \gamma(t) + \delta(t)] L^2 + 2(d-1)\delta(t) \frac{L^3 \rho}{L\rho + r_0 L^\alpha}.$$

We require that Q would be a real profile that depends only of ρ . Therefore, Setting $B = 0$ in Eq. (60) gives

$$\gamma(t) = \alpha \frac{L_t}{4L}. \quad (61)$$

Setting $C = 0$ and substituting (61) gives

$$\delta(t) = (1 - \alpha) \frac{L_t}{4L}. \quad (62)$$

Substitution of (61) and (62) in (59) gives rise to the new ring asymptotic profile

$$\psi_Q = \frac{1}{L^{1/\sigma}} Q(\rho) e^{i\tau + i\alpha \frac{L_t}{4L} r^2 + i(1-\alpha) \frac{L_t}{4L} (r - r_m(t))^2}, \quad (63a)$$

where

$$\tau = \int_0^t \frac{ds}{L^2(s)}, \quad \rho = \frac{r - r_m(t)}{L}, \quad r_m(t) = r_0 L^\alpha(t), \quad (63b)$$

and Q is the solution of

$$Q_{\rho\rho} + \frac{(d-1)L}{L\rho + r_0 L^\alpha} Q_\rho - Q + |Q|^{2\sigma} Q + A Q + iD Q = 0, \quad (64a)$$

with

$$A = -\frac{1}{4} [(L^3 \rho^2 + 2\alpha r_0 L^{2+\alpha} \rho + \alpha r_0^2 L^{1+2\alpha}) L_{tt} - \alpha(1-\alpha)r_0(r_0 L^{2\alpha} + 2L^{\alpha+1} \rho) L_t^2],$$

$$D = \frac{d-1}{2} \left[\alpha - \frac{2-\sigma}{\sigma(d-1)} + (1-\alpha) \frac{L\rho}{L\rho + r_0 L^\alpha} \right] L L_t. \quad (64b)$$

As noted, α expresses the relation between the ring width L and radius $r_m(t)$. We now discuss the possible values of α :

- $\alpha = 1$: In this case, the new phase term in (63) vanishes, hence (63) reduces to (56). Since $r_m(t) = r_0 L$, this case

corresponds to equal-rate collapse, e.g. the ψ_G ring solutions of the critical NLS (Section 2).

- $\alpha = 0$: In this case, the “old” phase term disappears. Since $r_m(t) \equiv r_0$, this case describes a standing ring solution, e.g. Raphael’s standing ring solutions ψ_P , see (40), of the supercritical quintic NLS (Section 3).

- $\alpha > 1$: In this case,

$$\rho = \frac{r - r_0 L^\alpha}{L} \approx \frac{r}{L}, \quad L \rightarrow 0.$$

Therefore, this case does not describe ring solutions, but rather the familiar singular peak solutions of the NLS.

- $\alpha < 0$: In this case, $r_m(t) \rightarrow \infty$, hence the ring power (L^2 norm) becomes infinite, see Appendix F. Since the power is conserved, there are no ring solutions in this case.
- $0 < \alpha < 1$: In this case, both the “old” term $\alpha \frac{L_t}{4L} r^2$ and the new phase term $(1-\alpha) \frac{L_t}{4L} (r - r_0 L^\alpha)^2$ affect the blowup dynamics. Since $r_m(t) = r_0 L^\alpha$, the ring radius shrinks to zero, but at a slower rate than the rate of the ring width L .

Therefore, we have the following result:

Lemma 8. *Let ψ be a singular ring solution of the NLS (55) with an asymptotic blowup profile $\psi(t, r) \sim \psi_Q(t, r)$, where ψ_Q is given by (63), and Q is a ring profile. Then, $0 \leq \alpha \leq 1$.*

4.1. Technical lemmas

The following lemmas will be needed for the analysis of supercritical rings in Sections 4.2–4.4.

Lemma 9. *The boundary conditions for a ring solution of Eq. (64) are*

$$\begin{cases} Q'(\rho = -r_0) = 0, & Q(\infty) = 0 & \alpha = 1, \\ Q'(\rho = -\infty) = 0, & Q(\infty) = 0 & 0 \leq \alpha < 1. \end{cases}$$

In addition, since the location of the ring peak is at $\rho = 0$:

$$Q'(0) = 0, \quad Q(0) \neq 0.$$

Proof. See Appendix B. \square

Lemma 10. *A necessary condition for the solvability of equation*

$$u''(\rho) - u + |u|^{2\sigma} u = \varepsilon[(a + bi)u + c\rho u'], \quad (65)$$

$$u(0) \neq 0, \quad u'(0) = 0, \quad u(\infty) = 0, \quad u'(-\infty) = 0,$$

where $a, b, c, \varepsilon \in \mathbb{R}$ and $0 < |\varepsilon| \ll 1$, is $b = 0$.

Proof. See Appendix D. \square

In what follows, we will also assume that near the singularity, $L(t)$ decays as $(T_c - t)^p$ or slightly faster (e.g. with a loglog correction term):

Conjecture 11. *The blowup rate $L(t)$ satisfies*

$$L \sim f_c(t)(T_c - t)^p, \quad L_t \sim f_c(t) \frac{d}{dt} [(T_c - t)^p],$$

$$L_{tt} \sim f_c(t) \frac{d^2}{dt^2} [(T_c - t)^p],$$

as $t \rightarrow T_c$, where

$$\lim_{t \rightarrow T_c} \frac{f_c(t)}{(T_c - t)^\varepsilon} = \infty$$

for any $\varepsilon > 0$.

4.2. Case $\alpha = 0$: Standing rings

We now prove the following:

Lemma 12. *Let ψ be a singular ring solution of the NLS (55) with an asymptotic blowup profile $\psi(t, r) \sim \psi_Q(t, r)$, where ψ_Q is given by (63) with $Q = Q(\rho) \in \mathbb{R}$, and assume that Conjecture 11 holds. Let $\alpha = 0$. Then,*

- (1) $\sigma = 2$.
- (2) The blowup rate $L(t)$ is equal to or faster than $\sqrt{T_c - t}$.

Proof. When $\alpha = 0$, by Eq. (64) and Lemma 9, the equation for Q is

$$Q''(\rho) + (d-1) \frac{L}{L\rho + r_0} Q_\rho - Q + |Q|^{2\sigma} Q + A Q + iDQ = 0, \quad (66)$$

$$A = -\frac{1}{4} L^3 L_{tt} \rho^2,$$

$$D = \frac{d-1}{2} \left[-\frac{2-\sigma}{\sigma(d-1)} + \frac{L\rho}{L\rho + r_0} \right] LL_t,$$

where

$$Q(0) \neq 0, \quad Q'(0) = 0, \quad Q'(-\infty) = 0, \\ Q(\infty) = 0. \quad \square$$

By Conjecture 11, $L^3 L_{tt} \sim p(p-1) f_c^4 (T_c - t)^{4(p-1/2)}$. Therefore, $A = -\frac{1}{4} L^3 L_{tt} \rho^2$ is bounded only if $p \geq \frac{1}{2}$, hence the blowup rate $L(t)$ is equal to or faster than $\sqrt{T_c - t}$.

Since $\lim_{t \rightarrow T_c} L = 0$,

$$D \sim D^{(0)} = -\frac{2-\sigma}{2\sigma} LL_t, \quad t \rightarrow T_c. \quad (67)$$

From the requirement that Q would be a real profile, it follows that D , hence $D^{(0)}$, should go to zero as $t \rightarrow T_c$.

- (1) If the blowup rate is a square root, i.e. $\lim_{t \rightarrow T_c} \frac{L}{\sqrt{T_c - t}} = f_c > 0$, then $D^{(0)} \sim \frac{2-\sigma}{2\sigma} \frac{f_c^2}{2}$. Therefore, from the requirement that $D^{(0)}$ should go to zero, it follows that $\sigma = 2$.
- (2) If the blowup rate is faster than a square root, then $\varepsilon(t) = LL_t \rightarrow 0$. Therefore

$$\lim_{t \rightarrow T_c} D = \lim_{t \rightarrow T_c} D^{(0)} = 0.$$

Let us consider the solvability of Eq. (66). We first show that, to leading order, Eq. (66) reduces to

$$Q''(\rho) - Q + |Q|^{2\sigma} Q = i \frac{2-\sigma}{2\sigma} \varepsilon(t) Q, \\ -\infty < \rho < \infty \quad (68)$$

subject to (see Lemma 9)

$$Q(0) \neq 0, \quad Q'(0) = 0, \quad Q'(-\infty) = 0, \\ Q(\infty) = 0.$$

Indeed, from a dimensional argument it follows that $A = \mathcal{O}(\varepsilon^2(t)) \ll \varepsilon(t)$. In addition, since the blowup rate is faster than a square root, $\lim_{t \rightarrow T_c} L_t = -\infty$. Therefore

$$(d-1) \frac{L}{L\rho + r_0} = \mathcal{O}(L) \ll LL_t = \varepsilon(t).$$

Hence, to leading order, Eq. (66) reduces to (68). By Lemma 10, Eq. (68) is solvable only if its right-hand side vanishes. Therefore, $\sigma = 2$. \square

Lemma 12 shows that:⁸

Corollary 13. *Standing ring solutions ($\alpha = 0$) of the form (63) exist only for $\sigma = 2$.*

We now show that the opposite direction is also true.

Lemma 14. *Let ψ be a singular ring solution of the NLS (55) with an asymptotic blowup profile $\psi(t, r) \sim \psi_Q(t, r)$, where ψ_Q is given by (63) and $Q = Q(\rho) \in \mathbb{R}$. In addition, assume that Conjecture 11 holds. If $\sigma = 2$ then $\alpha = 0$.*

Proof. By Lemma 8, $0 \leq \alpha \leq 1$. We will see in Lemma 20 that $\alpha = \frac{2-\sigma}{\sigma(d-1)}$ for $0 \leq \alpha \leq 1$. Therefore, $\sigma = 2$ implies $\alpha = 0$. \square

The question whether when $\sigma = 2$ the blowup rate is faster than or equal to $\sqrt{T_c - t}$ is not answered by Lemma 12. By Theorem 5, when $d = 2$ the blowup rate is given by the loglog law. In addition, our numerical simulations in Section 6 for $d = 1.5$ (See Fig. 21), as well as additional simulation for $d = 2.1$ and $d = 3$ (data not shown), suggest that the blowup rate is slightly faster than a square root. Moreover, since the arguments used in Section 3.2 can be applied with any $d > 1$, this suggests that the blowup rate is given by the loglog law for any $d > 1$.

Conjecture 15. *Let ψ be a singular ring solution of the quintic NLS*

$$i\psi_t(t, r) + \psi_{rr} + \frac{d-1}{r} \psi_r + |\psi|^4 \psi = 0, \quad (69)$$

such that the conditions of Lemma 14 hold. Then, the blowup rate is given by the loglog law (10).

Lemmas 12 and 14 together with Conjecture 15 imply that

Proposition 16. *Let ψ be a singular solution of the NLS (55) with an asymptotic blowup profile $\psi(t, r) \sim \psi_Q(t, r)$, where ψ_Q is given by (63) and $Q = Q(\rho) \in \mathbb{R}$. Let $\sigma = 2$ and assume that Conjecture 15 holds. Then,*

- (1) $\alpha = 0$.
- (2) The blowup rate is given by the loglog law (10).

⁸ Standing ring solutions also exist in the case $\sigma > 2$ but they are not of the form (63), see Section 9.

(3) The self-similar profile Q is given by (40).

Proposition 16 shows that standing ring solutions exist in the quintic NLS (69) for any $d > 1$. Therefore, Proposition 16 extends Theorem 5 which proved the existence of standing ring solutions only for $d = 2$. Indeed, the result of Proposition 16 can be motivated using *identical* arguments to the one we used to motivate Theorem 5 in Section 3.2.

Remark 17. Proposition 16 also suggests the existence of multibump standing ring solutions of the quintic NLS (69). Indeed, let us consider two collapsing standing rings $\psi_Q^{(1)}$ and $\psi_Q^{(2)}$ with corresponding radii $r_m^{(1)}(T_c^{(1)}) \ll r_m^{(2)}(T_c^{(2)})$. Let us construct the initial condition

$$\psi_0(r) = \psi_Q^{(1)}(T_c^{(1)} - \gamma, r) + (1 + \varepsilon)\psi_Q^{(2)}(T_c^{(2)} - \gamma, r),$$

where γ is smaller than $T_c^{(1)}$ and $T_c^{(2)}$. Since the coupling between the two rings is exponentially small, they each collapse at $t^{(i)} \approx \gamma$. Therefore, a proper choice of ε can give rise to a double ring solution for which both rings blow up at the same time. Similarly, a multibump solution with more than two rings can be constructed.

4.3. Case $\alpha = 1$: Ring solutions in the critical NLS

When $\alpha = 1$, the new asymptotic form (63) reduces to (56) and the solution undergoes equal-rate collapse. The following lemma characterizes all singular ring solutions in this case:

Lemma 18. Let ψ be a singular ring solution of the NLS (55) with an asymptotic blowup profile $\psi(t, r) \sim \psi_Q(t, r)$, where ψ_Q is given by (63) and $Q = Q(\rho) \in \mathbb{R}$, and assume that Conjecture 11 holds. Let $\alpha = 1$. Then

- (1) $\sigma d = 2$.
- (2) The blowup rate $L(t)$ is equal to $\sqrt{T_c - t}$.

Proof. When $\alpha = 1$, by Eq. (64) and Lemma 9,

$$Q''(\rho) + \frac{d-1}{\rho+r_0}Q_\rho - Q + |Q|^{2\sigma}Q + AQ + iDQ = 0, \quad (70)$$

$$Q(0) \neq 0, \quad Q'(0) = 0, \quad Q'(-r_0) = 0, \\ Q(\infty) = 0,$$

where

$$A = -\frac{1}{4}L^3L_{tt}(\rho+r_0)^2, \quad D = \frac{\sigma d - 2}{2\sigma}LL_t.$$

By Conjecture 11, $L^3L_{tt} \sim p(p-1)f_c^4(T_c-t)^{4(p-1/2)}$. Therefore, $A = -\frac{(\rho+r_0)^2}{4}L^3L_{tt}$ is bounded only if $p \geq \frac{1}{2}$, hence the blowup rate $L(t)$ is equal to or faster than $\sqrt{T_c-t}$.

If the blowup rate is faster than a square root, then $LL_t \rightarrow 0$. Therefore, as $t \rightarrow T_c$, Eq. (70) reduces to

$$Q''(\rho) + \frac{d-1}{\rho+r_0}Q_\rho - Q + |Q|^{2\sigma}Q = 0, \quad (71)$$

$$Q(0) \neq 0, \quad Q'(0) = 0, \quad Q'(-r_0) = 0, \\ Q(\infty) = 0,$$

Under the transformation $\tilde{\rho} = \rho + r_0$ and $R(\tilde{\rho}) = Q(\rho)$, Eq. (71) becomes Eq. (5) with the additional constraint that $R'(\tilde{\rho} = r_0) = 0$. However, Eq. (5) does not admit ring solutions, see Appendix C. Therefore, although the excited states $\{R^{(n)}\}_{n=1}^\infty$ of this equation may fulfill the additional constraint, none of them are ring solutions. Hence the blowup rate cannot be faster than a square root.

From the requirement that Q is a real profile, it follows that D should go to zero as $t \rightarrow T_c$. Since the blowup rate is a square root, i.e. $L/\sqrt{T_c-t} \sim f_c > 0$, then $D \sim \frac{2-\sigma d}{2\sigma} \frac{f_c^2}{2}$. Therefore, from the requirement that D should go to zero, it follows that $\sigma d = 2$. \square

Lemma 18 proves that

Corollary 19. Singular ring solutions whose asymptotic profile is given by (56) exist only in the critical NLS.

This result explains why attempts to find stable equal-rate ring solutions of the form (56) in the supercritical NLS (see, e.g. [25]) did not succeed.

The opposite direction, i.e. that ring solutions of the critical NLS undergo equal-rate collapse ($\alpha = 1$) was already proved in Proposition 4.

4.4. Case $0 < \alpha < 1$: Ring solutions in the supercritical NLS ($2/d < \sigma < 2$)

Lemma 20. Let ψ be a singular ring solution of the NLS (55) with an asymptotic blowup profile $\psi(t, r) \sim \psi_Q(t, r)$, where ψ_Q is given by (63) and $Q = Q(\rho) \in \mathbb{R}$. In addition, assume that Conjecture 11 holds. Let $0 < \alpha < 1$. Then,

- (1)
$$\alpha = \frac{2-\sigma}{\sigma(d-1)}. \quad (72)$$

- (2) The blowup rate $L(t)$ is equal to or faster than $(T_c-t)^{\frac{1}{1+\alpha}}$.

Proof. As we have seen, the equation for Q is given by (64). By Conjecture 11, as $t \rightarrow T_c$,

$$A \sim -\frac{\alpha r_0^2}{4} \left[L^{2\alpha+1}L_{tt} - (1-\alpha)L^{2\alpha}L_t^2 \right] \\ = -\frac{\alpha r_0^2}{4} p(\alpha p - 1) f_c^{2(1+\alpha)} (T_c - t)^{2((\alpha+1)p-1)}.$$

Therefore, A is bounded as $t \rightarrow T_c$ only if $p \geq \frac{1}{1+\alpha}$, hence the blowup rate $L(t)$ is equal to or faster than $(T_c-t)^{\frac{1}{1+\alpha}}$, i.e.,

$$L(t) \sim f_c(T_c-t)^{\frac{1}{1+\alpha}}, \quad f_c \geq 0. \quad (73)$$

In particular, the blowup rate is faster than a square root, hence $\lim_{t \rightarrow T_c} LL_t = 0$.

Since $\lim_{t \rightarrow T_c} L = 0$,

$$D \sim D^{(0)} = \frac{d-1}{2} \left[\alpha - \frac{2-\sigma}{\sigma(d-1)} \right] LL_t, \quad t \rightarrow T_c. \quad (74)$$

The requirement that Q is real is satisfied, since $LL_t \rightarrow 0$ implies that

$$\lim_{t \rightarrow T_c} D = \lim_{t \rightarrow T_c} D^{(0)} = 0.$$

Let us consider the solvability of Eq. (64). We first show that, to leading order, Eq. (64) reduces to

$$\begin{aligned} Q''(\rho) - \left[1 + \frac{\alpha r_0^2}{4(1+\alpha)^2} f_c^{2(1+\alpha)} \right] Q + |Q|^{2\sigma} Q \\ = \left[\frac{d-1}{r_0} Q' - \frac{\alpha}{2(1+\alpha)^2} f_c^{2(1+\alpha)} \rho Q \right. \\ \left. - i \frac{d-1}{2} \left(\alpha - \frac{2-\sigma}{\sigma(d-1)} \right) Q \right] \varepsilon(t), \\ -\infty < \rho < \infty \end{aligned} \quad (75)$$

where $\varepsilon(t) = L^{1-\alpha}$, subject to (see Lemma 9)

$$Q(0) \neq 0, \quad Q'(0) = 0, \quad Q(\infty) = 0, \\ Q'(-\infty) = 0.$$

Indeed, from a dimensional argument it follows that

$$L^3 L_{tt} = \varepsilon^2(t) \ll \varepsilon(t).$$

Hence, substituting (73) into A of Eq. (64b) gives

$$A = -\frac{\alpha f_c^{2(1+\alpha)}}{2(1+\alpha)^2} \left[\frac{r_0^2}{2} - \rho \varepsilon(t) \right] + \mathcal{O}(\varepsilon^2).$$

By Lemma 10, Eq. (75) is solvable only if

$$\frac{d-1}{2} \left(\alpha - \frac{2-\sigma}{\sigma(d-1)} \right) = 0,$$

from which relation (72) follows. Finally, as $t \rightarrow T_c$, Eq. (64) reduces to Eq. (78). \square

By Lemma 8, $0 \leq \alpha \leq 1$. Since relation (72) for α is a one-to-one relation, the opposite direction of Lemma 20 immediately follows:

Lemma 21. *Let ψ be a singular ring solution of the NLS (55) with an asymptotic blowup profile $\psi(t, r) \sim \psi_Q(t, r)$, where ψ_Q is given by (63) and $Q = Q(\rho) \in \mathbb{R}$. Let $2/d < \sigma < 2$. Then, α is given by (72).*

The question whether the blowup rate is faster than or equal to $(T_c - t)^{\frac{1}{1+\alpha}}$ is not answered by Lemma 20. However, the numerical simulations of Section 6.1 suggest that

Conjecture 22. *Let ψ be a singular solution of the NLS (55) with an asymptotic blowup profile (63), where $0 < \alpha < 1$. Then, the blowup rate L is equal to $(T_c - t)^{\frac{1}{1+\alpha}}$.*

From Lemma 21 and Conjecture 22 we have the following result:

Proposition 23. *Let ψ be a singular solution of the NLS (55) with an asymptotic blowup profile $\psi(t, r) \sim \psi_Q(t, r)$, where ψ_Q is given by (63). Let $2/d < \sigma < 2$ and assume that Conjecture 22 holds. Then*

(1)

$$\alpha = \frac{2-\sigma}{\sigma(d-1)}.$$

(2) *The blowup rate is $\frac{1}{1+\alpha}$, i.e.,*

$$\lim_{t \rightarrow T_c} \frac{L(t)}{(T_c - t)^{\frac{1}{1+\alpha}}} = f_c > 0. \quad (76)$$

(3) *The self-similar profile Q is given by*

$$Q(\rho; \sigma) = \omega^{\frac{1}{\sigma}} (1 + \sigma)^{\frac{1}{2\sigma}} [\operatorname{sech}(\omega \sigma \rho)]^{\frac{1}{\sigma}}, \quad (77)$$

which is the solution of

$$Q_{\rho\rho} - \omega^2 Q + Q^{2\sigma+1} = 0, \quad (78)$$

where

$$\omega = \sqrt{1 - \frac{\alpha r_0^2}{4(1+\alpha)^2} f_c^{2(1+\alpha)}}. \quad (79)$$

The result of Proposition 23 is very surprising in light of the “success” of the motivation for Theorem 5 and for Proposition 16, see Sections 3.2 and 4.2. Indeed, for collapsing ring solutions of the form (63), the ring radius $r_m(t) = \mathcal{O}(L^\alpha)$, and $\psi_r(r) = \mathcal{O}(L^{-(1+\sigma)})$, in the ring region $r \approx r_m(T_c)$. Therefore $\frac{d-1}{r} \psi_r = \mathcal{O}(L^{-(\alpha+1+\sigma)})$ and $\psi_{rr} = \mathcal{O}(L^{-(2+\sigma)})$. As a result, when $0 < \alpha < 1$ the $\frac{d-1}{r} \psi_r$ term in Eq. (55) becomes negligible compared with ψ_{rr} as $t \rightarrow T_c$. Hence, near the singularity, the d -dimensional NLS (55) can be expected to “reduce” to the one-dimensional NLS

$$i\psi_t(t, r) + \psi_{rr} + |\psi|^{2\sigma} \psi = 0. \quad (80)$$

However, for $2/d < \sigma < 2$, this is a subcritical one-dimensional NLS, whose solutions do not become singular. Therefore, although the $\frac{d-1}{r} \psi_r$ term becomes smaller and smaller than the other terms as the solution collapses, it cannot be neglected near the singularity.

5. Strong collapse ($2/d \leq \sigma < 2$)

Let us define the power that collapses into the ball $r < \varepsilon$ as

$$P_\varepsilon(t) = \int_{r < \varepsilon} |\psi(t, r)|^2 r^{d-1} dr.$$

The power that collapses into the singularity point at $r = 0$ can be defined as⁹

$$P_{\text{collapse}} = \inf_\varepsilon \lim_{t \rightarrow T_c} P_\varepsilon(t). \quad (81)$$

It is customary to distinguish between two cases:

- (1) *Strong collapse*, in which the amount of power collapsing into the singularity is positive, i.e. $P_{\text{collapse}} > 0$;
- (2) *Weak collapse*, in which the amount of power collapsing into the singularity is zero, i.e. $P_{\text{collapse}} = 0$.

⁹ Definition (81) does not apply to standing ring solutions ($\sigma = 2$), since they concentrate power on a sphere and at not a point.

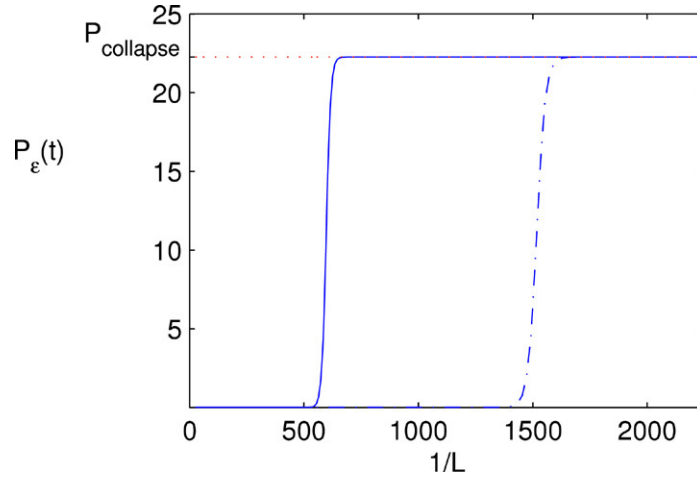


Fig. 16. $P_\varepsilon(t)$ as a function of the focusing level $1/L$ for the solution of Fig. 18: $\varepsilon = 0.1$ (solid), $\varepsilon = 0.05$ (dash-dots). Dotted curve is $P_{\text{collapse}} = r_0^{d-1} \int_{-\infty}^{\infty} Q^2 dr \approx 22.477 P_{\text{cr}}$.

It has been known that singular solutions of the critical NLS undergo strong collapse, whereas singular solutions of the supercritical NLS undergo weak collapse [3]. However, these characterizations were only for singular peak solution. We now show that this is *not* the case for collapsing ring solutions. Rather, both critical and supercritical ring solutions undergo strong collapse.

Lemma 24. *Let ψ be a singular solution of the NLS (55) with an asymptotic blowup profile $\psi(t, r) \sim \psi_Q(t, r)$, where ψ_Q is given by (63). Then*

$$P_{\text{collapse}} = \begin{cases} \|\psi_Q^0\|_2^2 & \sigma = 2/d, \\ r_0^{d-1} \int_{-\infty}^{\infty} Q^2 d\rho & 2/d < \sigma < 2. \end{cases} \quad (82)$$

In particular, ψ undergoes strong collapse.

Proof. See Appendix E. \square

Remark. In Section 2 we saw that in the critical case $\sigma = 2/d$, the self-similar profile Q is given by G , the solution of (31). We also noted that the collapse is only quasi self-similar, see Eq. (34). Therefore, although the solution of (31) has an infinite power (L_2 norm), the slowly-decaying, infinite-power oscillatory tail of the G profile is “irrelevant” to the critical NLS ring solution [26]. Hence, $\|\psi_Q^0\|_2^2$ in (82) corresponds to the power of the G profile in the ring region, i.e. $\int_{\rho_1-r_0}^{\rho_2-r_0} G^2(\rho+r_0)(\rho+r_0)^{d-1} d\rho$.

In the critical NLS, singular peak-type solutions that collapse with the ψ_R profile (8) undergo strong collapse with $P_{\text{collapse}} = P_{\text{cr}}$, independently of the initial condition. In contrast, in the case of singular ring solutions, P_{collapse} depends on the initial condition and increases as a function of the initial power. Therefore, ring collapse is more efficient than “peak collapse”, in the sense that it concentrates a larger fraction of the initial power into the singularity. For example, a Gaussian initial condition with power equal to $40P_{\text{cr}}$ collapses

with the ψ_R profile, hence only 2.5% of its initial power collapses into the singularity. In contrast, a super-Gaussian initial condition with the same initial power collapses with a ring profile that concentrates 70% of the initial power into the singularity [26].

This difference is even more dramatic in the supercritical NLS, since in this case $P_{\text{collapse}} = 0$ for “peak-type” solutions, while $P_{\text{collapse}} > 0$ for ring solutions. For example, in Fig. 16 we plot $P_{\varepsilon=0.1}$ in the case $\sigma = 1.1$ and $d = 2.1$ ($\alpha \approx 0.7438$) for the initial condition $\psi_0 = 1.02\psi_Q^0$, where ψ_Q^0 is given by (84). Initially, $r_m(t) \gg 0.1$ and $P_{\varepsilon=0.1} \ll 1$. However, once $r_m(t) \ll 0.1$, $P_{\varepsilon=0.1} \approx 41.491 = 22.276 P_{\text{cr}}$. In Fig. 16 we also plot $P_{\varepsilon=0.05}$. In this case the initial stage when $P_{\varepsilon=0.05} \ll 1$ is longer, since $r_m(t) \approx 0.05$ at a later stage of the focusing. However, once $r_m(t) \ll 0.05$, $P_{\varepsilon=0.05}$ approaches the same value of $\approx 22.276 P_{\text{cr}}$, showing that $P_{\text{collapse}} \approx 22.276 P_{\text{cr}}$. The initial power of the solution is $P(0) = \|\psi_0\|_2^2 = 22.733 P_{\text{cr}}$, hence 98% of the initial power collapses into the singularity.¹⁰

6. Numerical investigations

We now present numerical investigations of supercritical and critical ring solutions of Eq. (55) for $0 \leq \alpha \leq 1$.

6.1. $0 < \alpha < 1$

We first present a systematic study of the following two-ring solutions in the case $0 < \alpha < 1$:

(1) $\sigma = 1.1$ and $d = 2.1$. The expected value of α is from Eq. (72),

$$\alpha = \frac{2 - 1.1}{1.1(2.1 - 1)} = \frac{90}{121} \approx 0.74380. \quad (83a)$$

¹⁰ To confirm the agreement with (82), we first extract r_0 . For this choice of ψ_Q^0 , $L_0 = \frac{1}{2\sigma}$ and $r_0 L_0^\alpha = 5$, therefore, $r_0 = \frac{5}{L_0^\alpha} = 5 \cdot 2^{\alpha\sigma} \approx 8.887$. Hence by (82), $P_{\text{collapse}} = r_0^{d-1} \int_{-\infty}^{\infty} Q^2 dr \approx 41.864 = 22.477 P_{\text{cr}}$.

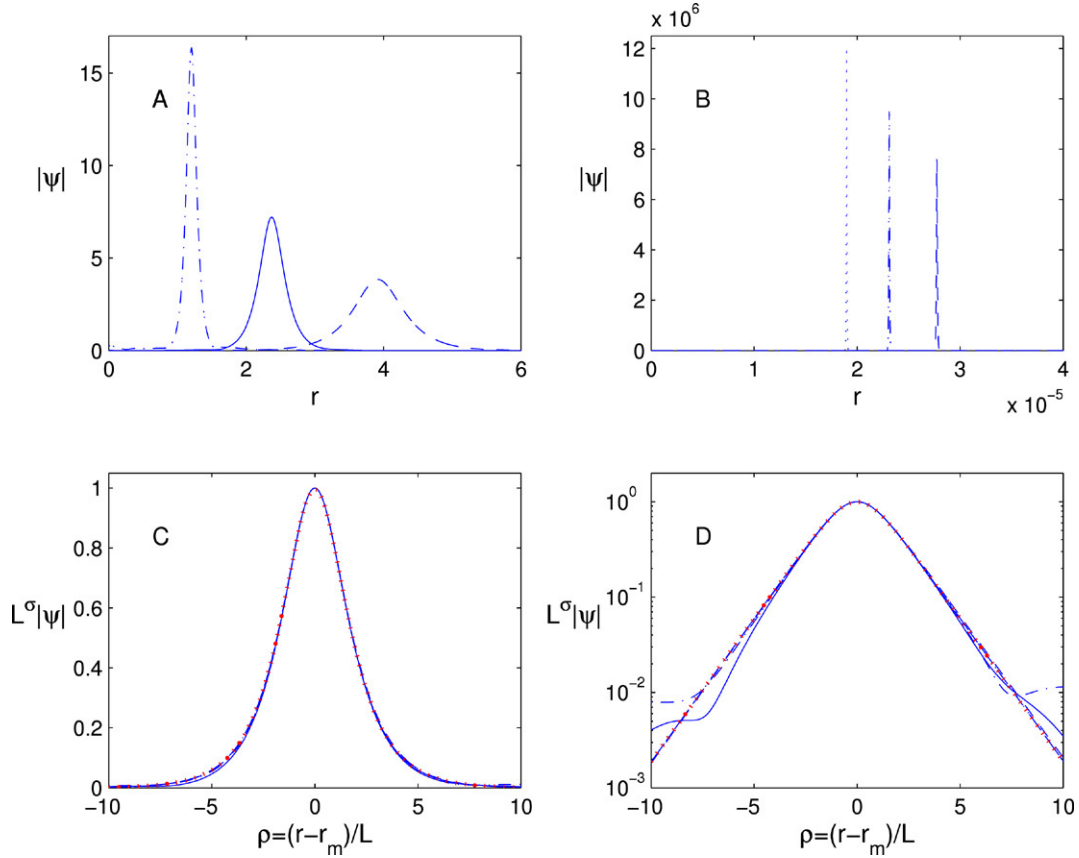


Fig. 17. Solution of Eq. (55) with $\sigma = 1.1$ and $d = 2.1$ and the initial condition (84) at: A: $t = 0.0723$, ($1/L = 4.40$, dashes), $t = 0.172$, ($1/L = 8.77$, solid) and $t = 0.238$, ($1/L = 21.63$, dash-dots), B: $1/L = 3.69 \times 10^7$ (dashes), $1/L = 4.72 \times 10^7$ (dash-dots) and $1/L = 6.15 \times 10^7$ (dots). Solution is so close to the singularity that for all three curves $t \approx T_c = 0.2659$ and the three times differ only in the 14th digits. C: The three curves from A and the three curves from B normalized according to (51), all six curves are nearly indistinguishable. The bold dotted curve is the asymptotic profile Q (77) D: Same data as in C on a semilogarithmic scale.

(2) $\sigma = 1.25$ and $d = 3$. The expected value of α is

$$\alpha = \frac{2 - 1.25}{1.25(3 - 1)} = \frac{3}{10}. \quad (83b)$$

We use the initial condition $\psi_Q(0) = \psi_Q^0$, see Eq. (63), with

$$L(0) = \frac{1}{2^\sigma}, \quad \frac{L_t(0)}{L(0)} = -4, \quad r_0 L^\alpha(0) = 5, \quad \omega = 1,$$

to obtain,

$$\psi_Q^0 = 2(1 + \sigma)^{1/2\sigma} [\operatorname{sech}(2^\sigma \sigma (r - 5))]^{1/\sigma} e^{-i\alpha r^2 - i(1-\alpha)(r-5)^2}. \quad (84)$$

The choice $L(0) = \frac{1}{2^\sigma}$ gives an initial condition which is sufficiently localized, so as to prevent a possible truncation of the sech ring tail near the origin.

We first present a simulation with $d = 2.1$ and $\sigma = 1.1$. Fig. 17A and B shows that the numerical solution indeed collapses with a ring profile up to focusing factors of $\mathcal{O}(10^7)$. In order to check for self-similarity we rescale the solution ψ according to (51). Fig. 17C shows that all rescaled plots of the solution at focusing levels varying from 10^1 to 10^7 are nearly indistinguishable, indicating that the solution is indeed self-similar while focusing over six orders of magnitude.

In addition, Fig. 17C also shows that the rescaled profile perfectly fits the Q profile (77). Plotting the same data on a semilogarithmic scale (Fig. 17D) shows that the solution is “only” quasi self-similar, i.e. the self-similar profile ψ_Q characterizes the collapsing ring region ($-5 \leq \rho \leq 5$) but not the inner and outer regions ($|\rho| \geq 5$).

Next, we calculate the parameter α of the ring radius shrinkage. According to Eq. (63), $r_m(t) = r_0 L^\alpha$ where $\alpha \approx 0.74380$, see Eq. (83a). To find the parameter α numerically, we calculate $r_m(t)$ from Eq. (51) and plot $r_m(t)$ as a function of $1/L$. Fig. 18A shows that $r_m(t) \approx 11.826206L^\alpha$ with $\alpha = 0.74391$, which differs from the predicted value of α by less than 0.015%.

We now consider the *blowup rate* of these solutions. According to Lemma 20 the blowup rate is either faster than or equal to $(T_c - t)^{\frac{1}{1+\alpha}}$. To determine numerically which of these two possibilities hold, we first plot the blowup rate L as a function of $T_c - t$ and find the best fitting exponent p for $L \sim f_c(T_c - t)^p$. The results in Fig. 18B show that $L \sim f_c(T_c - t)^{0.57342}$, perfectly fitting the expected value of $\frac{1}{1+\alpha} = 0.57346$ with a relative error of less than 0.007%. Since plotting L as a function of $T_c - t$ is not sensitive enough to tell a $\frac{1}{1+\alpha}$ blowup rate from a slightly-faster-than-a $\frac{1}{1+\alpha}$ blowup rate,

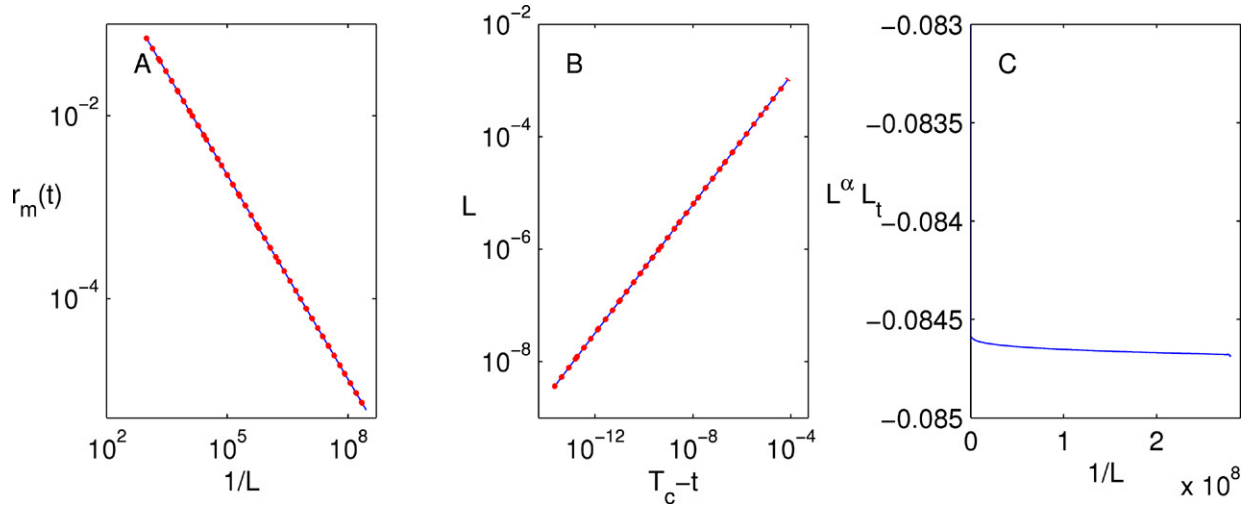


Fig. 18. Solution of Fig. 17. A: $r_m(t)$ as a function of L . Dotted curve is the fitted curve $cL(t)^{0.74391}$ where $c = 11.826206$. B: L as a function of $(T_c - t)$ on a logarithmic scale. Dotted curve is the fitted curve $L = c(T_c - t)^{0.57342}$ where $c = 0.24285$. C: $L^\alpha L_t$ as a function of $1/L$.

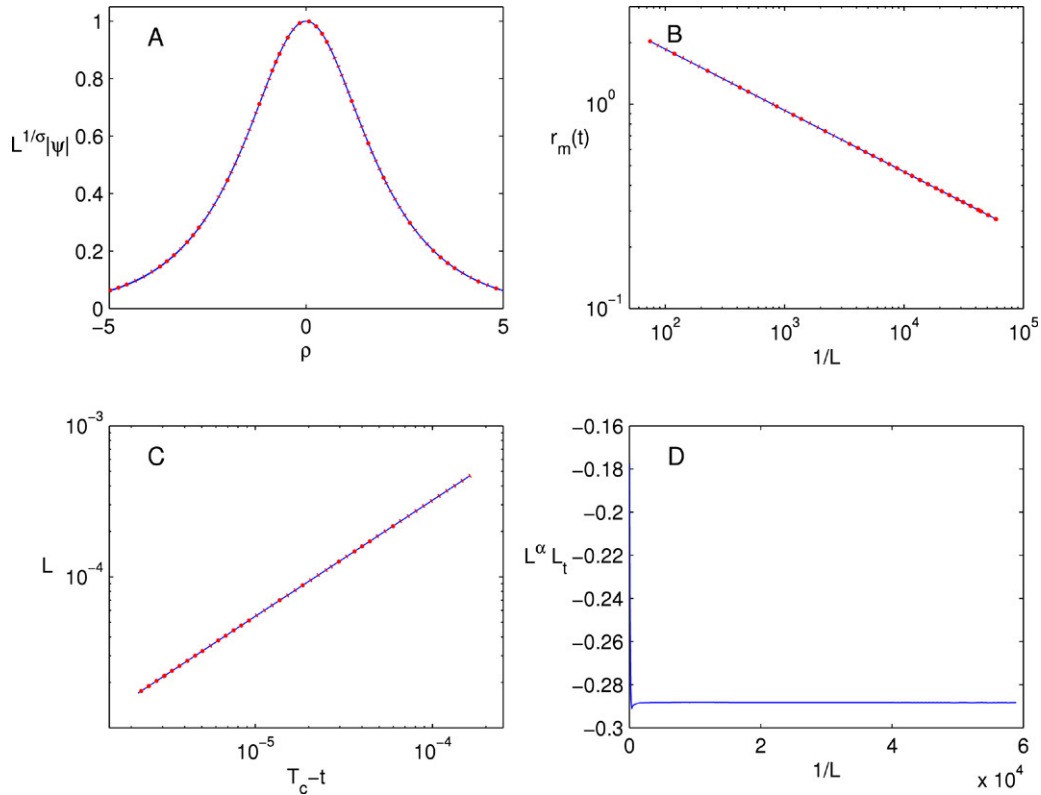


Fig. 19. Solution of Eq. (55) with $\sigma = 1.25$ and $d = 3$ ($\alpha = 0.3$) for the initial condition (84). A: Rescaled solution according to (51) at focusing levels $1/L = 171.8$, (solid), $1/L = 9789.5$, (dashed) and $1/L = 60619.23$, (dash-dots), dotted curve is the asymptotic profile Q (77), all curves are indistinguishable around the peak. B: $r_m(t)$ as a function of $1/L$. Dotted curve is the fitted curve $r_m(t) = cL^{0.300021}(t)$ where $c = 9.21$. C: L as a function of $(T_c - t)$ on a logarithmic scale. Dotted curve is the fitted curve $L = (T_c - t)^{0.76919}$ where $c = 0.383$. D: $L^\alpha L_t$ as a function of $1/L$.

we plot $L^\alpha L_t$ as a function of the focusing factor $1/L$. For a blowup rate equal to $\frac{1}{1+\alpha}$, $L^\alpha L_t$ goes to a negative constant, but for a blowup rate faster than $\frac{1}{1+\alpha}$, $L^\alpha L_t$ goes to zero. The results in Fig. 18C shows that $\lim_{t \rightarrow T_c} L^\alpha L_t = -0.0846$, indicating that $L \sim f_c \cdot (T_c - t)^{\frac{1}{1+\alpha}}$ with $f_c \approx 0.333$. Therefore, we conclude that the blowup rate is equal to $(T_c - t)^{\frac{1}{1+\alpha}}$.

Similar results are presented in Fig. 19 for the case of $d = 3$ and $\sigma = 1.25$. In this case, it follows from Lemma 20 that $r_m(t) = r_0 L^\alpha$ where $\alpha = 0.3$, and that the blowup rate L is faster than or equal to $(T_c - t)^{\frac{1}{1+\alpha}}$ where $\frac{1}{1+\alpha} \approx 0.7692$. Fitting $r_m(t)$ as a function of $1/L$ shows that $r_m(t) \approx r_0 L^\alpha$, where $\alpha = 0.30021$, see Fig. 19B. Plotting L as a function

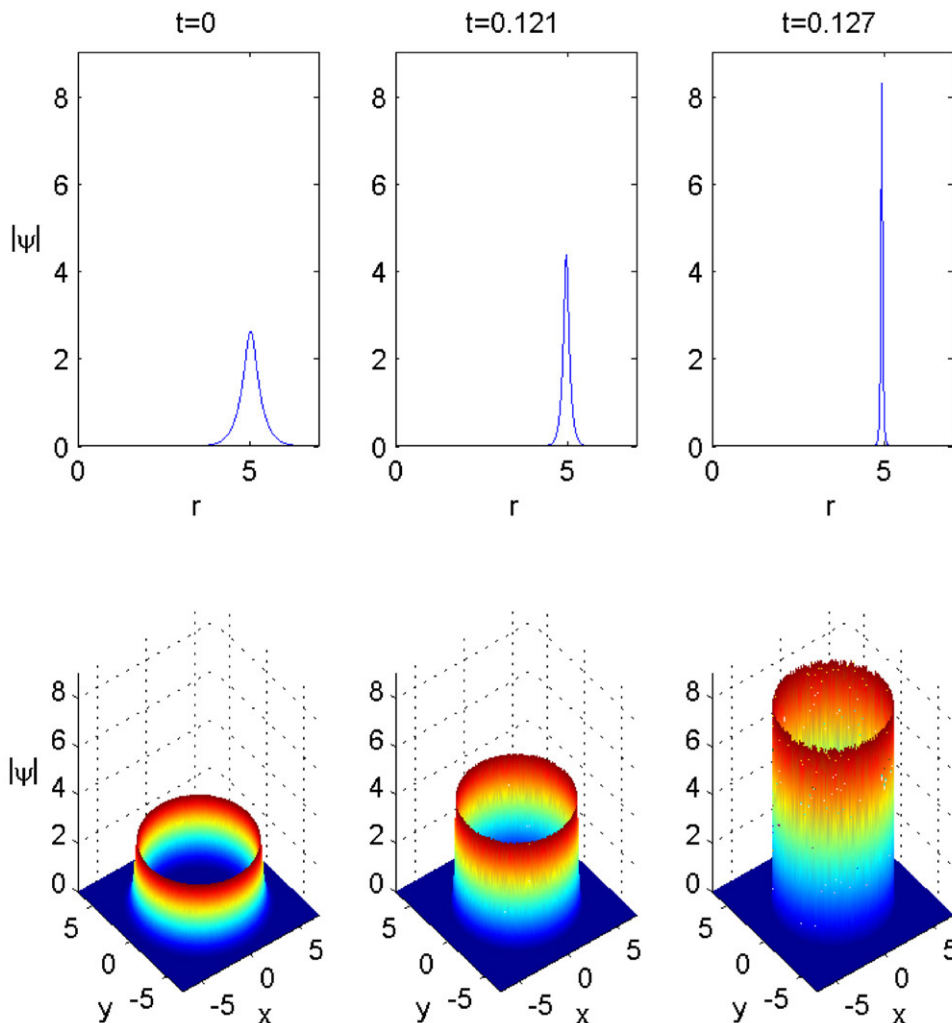


Fig. 20. Solution of the quintic NLS (69) with $d = 1.5$ and with ψ_0 given by (49).

of $(T_c - t)$ show that $L \sim f_c(T_c - t)^{0.76919}$. Therefore, the relative errors in the values of the shrinkage rate and the blowup rate are less than 0.04%. The results in Fig. 19D shows that $\lim_{t \rightarrow T_c} L^\alpha L_t = -0.286$, indicating that $L \sim f_c(T_c - t)^{\frac{1}{1+\alpha}}$ with $f_c \cong 0.584$. Therefore, we conclude that the blowup rate is equal to $(T_c - t)^{\frac{1}{1+\alpha}}$.

6.2. $\alpha = 0$

In Section 3 we presented a systematic numerical investigation of Raphael's standing ring solution, ψ_P , for $\sigma = 2$ and $d = 2$ (for which $\alpha = 0$). According to Lemma 14, ring solutions of the supercritical quintic NLS (69) collapse as standing ring solutions for any $d > 1$ and not just for $d = 2$. To see that, we now solve numerically the case $\sigma = 2$ and $d = 1.5$. In Fig. 20, we plot the early stages of the collapse as the solution focuses by a factor of ≈ 3 . As predicted by Lemma 14, as the ring amplitude increases and the ring width shrinks, the ring radius does not go to zero, but rather converges to a positive constant. To confirm that the collapse is self-similar according to (50), we rescale the solution ψ according to (51). Fig. 21A

shows that all rescaled plots of the solution at focusing levels varying from 10^1 to 10^5 are indistinguishable, indicating that the solution is indeed self-similar while focusing over 4 orders of magnitude. In addition, Fig. 21A shows that the rescaled profile perfectly fits the Q profile (77). Fig. 21B shows that the ring radius converge to $r_m(T_c) \approx 4.901$, indicating that the solution is a standing ring solution. According to Proposition 23 the blowup rate is $\sqrt{T_c - t}$ or faster. Indeed, Fig. 21C shows that $L \sim (T_c - t)^{0.49883}$. Plotting LL_t does not give a conclusive indication whether it goes to a negative constant or to zero, i.e. if the blowup rate is a square root blowup or slightly faster, see Fig. 21D. However, comparison with the benchmark cases of Fig. 5D and Fig. 12D suggests that the blowup rate is faster than a square root.

6.3. $\alpha = 1$

We have already presented systematic numerical investigations of equal-rate collapsing ring ($\alpha = 1$) in two cases:

- (1) $\sigma = 1$ and $d = 2$ in [26].
- (2) $\sigma = \frac{8}{7}$ and $d = \frac{7}{4}$ in Section 2.

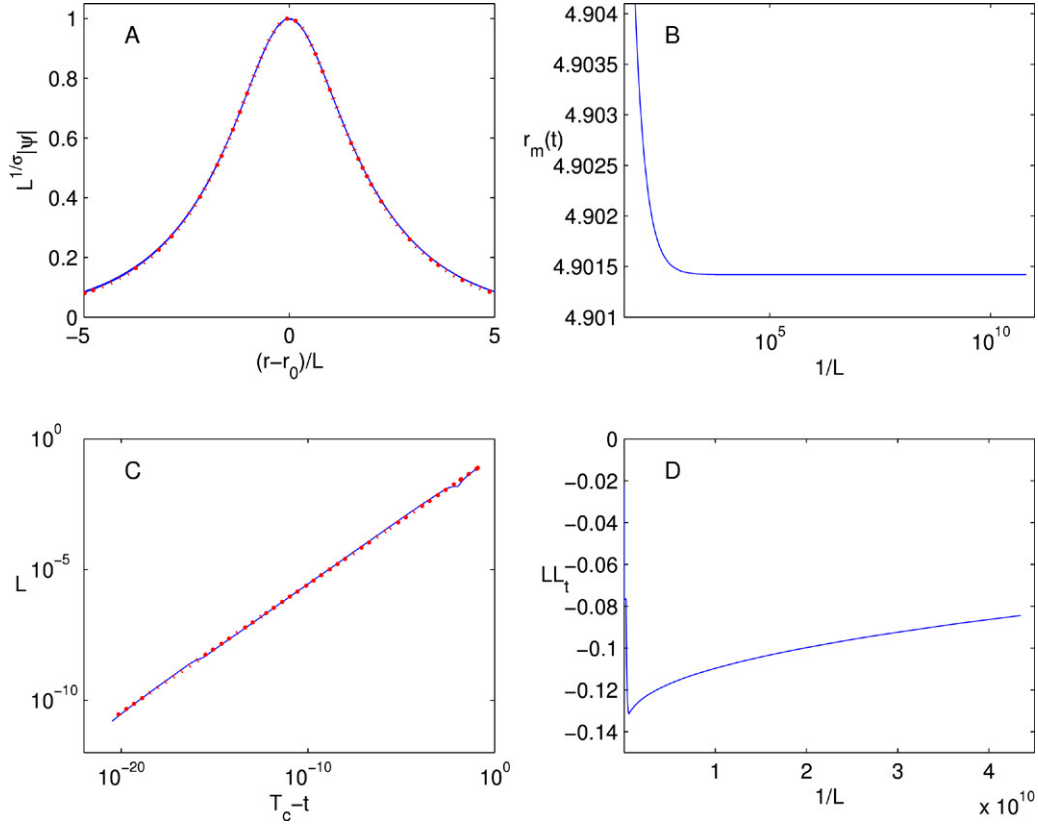


Fig. 21. Solution of the NLS (55) with $\sigma = 2$ and $d = 1.5$ ($\alpha = 0$) and the initial condition (84). A: Rescaled solution according to (51) at focusing levels $1/L = 19.04$ (solid), $1/L = 7.48 \times 10^5$ (dashed), and $1/L = 1.45 \times 10^{10}$ (dash-dots), dotted curve is the asymptotic profile Q (77), all four curves are indistinguishable around the peak. B: $r_m(t)$ as a function of $1/L$. C: L as a function of $(T_c - t)$ on a logarithmic scale. Dotted curve is the fitted curve $c(T_c - t)^{0.49883}$ where $c = 0.00041$. D: LL_t as a function of $1/L$.

6.4. Observation of radial phase

We have already observed the radial phase for the case $\alpha = 0$ in Fig. 11. We now consider the radial phase of supercritical ring solutions for $0 < \alpha < 1$. Our goal is to show that indeed, the phase of the solution is given by

$$S(r, t) = \frac{L_t}{4L} \left[\alpha r^2 + (1 - \alpha)(r - r_m(t))^2 \right], \quad (85)$$

or equivalently, by

$$S(\rho, t) = \frac{1}{4} LL_t \left[\rho^2 + \frac{2\alpha r_m(t)}{L} \rho + \frac{\alpha r_m^2(t)}{L^2} \right], \quad (86)$$

$$\rho = \frac{r - r_m(t)}{L}.$$

A-priori, this implies that the phase should consist of a parabola centred at $r = 0$ and another parabola centred at $r = r_m(t)$. However, as we have seen in Fig. 17, the collapse is only quasi self-similar, i.e. ψ_Q of Eq. (63) describes the solution only around the ring's peak. Accordingly, Eq. (85) is expected to describe the phase only around the ring peak at $r = r_m(t)$ and not near the origin at $r = 0$, i.e. for $\rho = \mathcal{O}(1)$ in (86).

To verify that the radial phase is given by (86), we compare the numerical phase $S_{\text{numerical}}$ with the phase $S_{\text{predicted}}$ predicted by (86), where L is recovered from the simulation (see Section 10.2 for more details) and $\alpha r_m^2(t)/L^2 = S_{\text{numerical}}(\rho =$

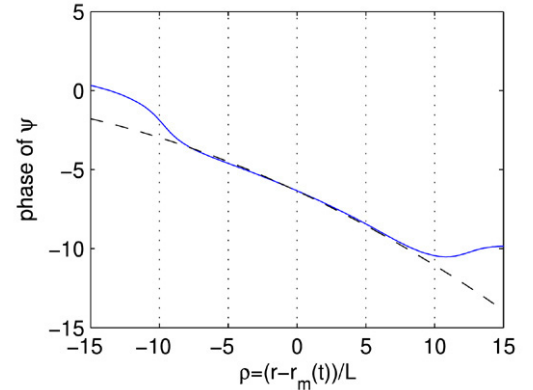


Fig. 22. Phase of the solution of Fig. 18 at $t = 0.263$ ($1/L = 92.03$). Dashed curve is $S_{\text{predicted}} = -0.0066(\rho^2 + 61.03\rho) - 6.352$.

$0, t)$. In Fig. 22 it can be seen that for $-5 \leq \rho \leq 5$, $S_{\text{numerical}}$ and $S_{\text{predicted}}$ are indistinguishable. The phase in this regime is nearly linear, since as $L \rightarrow 0$, the quadratic term in (86) becomes negligible, i.e.

$$\begin{aligned} S(\rho) - S(0) &\sim \frac{1}{4} LL_t \cdot \frac{2\alpha r_m(t)}{L} \rho = \frac{\alpha r_m(t) L_t}{2} \rho \\ &= \frac{\alpha r_0 L^\alpha L_t}{2} \rho \\ &\sim -\frac{\alpha f_c^{1+\alpha} r_0}{2(1+\alpha)} \rho. \end{aligned}$$

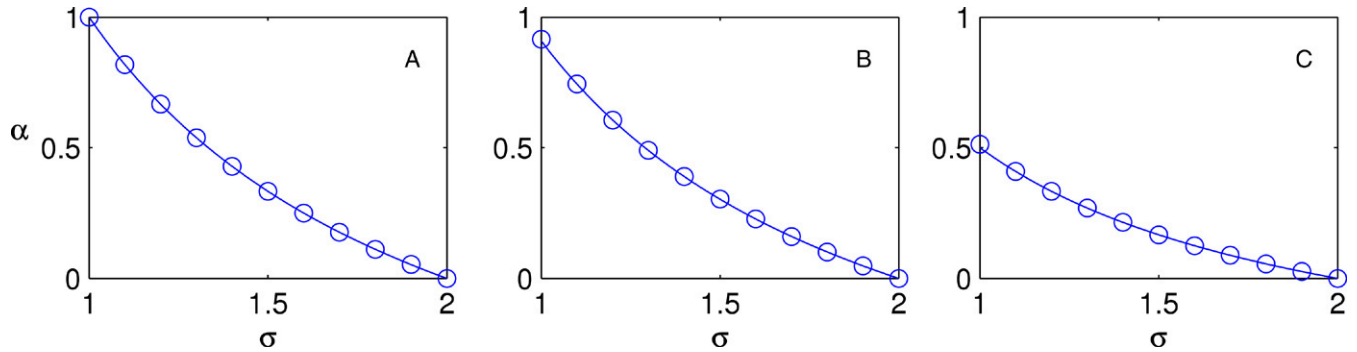


Fig. 23. Computed values of α (circles) for $\sigma = 1, 1.1, 1.2, \dots, 2$. Solid curve is Eq. (72). A: $d = 2$, B: $d = 2.1$, C: $d = 3$.

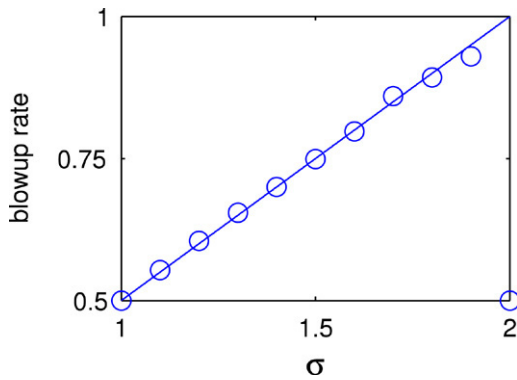


Fig. 24. Computed blowup rate (circles) for $d = 2$ and $\sigma = 1, 1.1, 1.2, \dots, 2$. Solid curve is $\frac{1}{1+\alpha}$.

Therefore, the slope of S is negative and asymptotically independent of t .

6.5. Numerical verification of Proposition 2 for the value of α

The prediction of Proposition 2 for the value of α was found to be in excellent agreement in all six simulations presented so far in this paper. We now systematically verify the validity of Proposition 2 for $d = 2$, $d = 2.1$ and $d = 3$ and for $\sigma = 1, 1.1, 1.2, \dots, 2$. Fig. 23 shows that in all 3×11 cases, the difference between the numerical value of α and the analytical predictions is less than 0.1%.

6.6. Numerical verification of Proposition 3 for the blowup rate

The six simulations presented so far in this paper perfectly agreed with the blowup rates predicted in Proposition 3. To validate the predicted blowup rates for a wider series of simulations, we run a series of simulations with $d = 2$ and $\sigma = 1, 1.1, 1.2, \dots, 2$. In the first 10 cases (for $\sigma < 2$) the blowup rate is $f_c(T_c - t)^p$, where the difference between p and $\frac{1}{1+\alpha}$ is less than 2%, see Fig. 24. In addition, in all these simulations, $L^\alpha L_t \rightarrow \text{Const} \neq 0$ (data not shown), showing that the blowup rate is $\frac{1}{1+\alpha}$ with no loglog-type corrections. When $\sigma = 2$, $p = 0.5001$ and $LL_t \rightarrow 0$, i.e. the blowup rate is slightly faster than a square root. The jump discontinuity in the blowup rate at $\sigma = 2$ follows from Proposition 3.

7. Super-Gaussian initial condition

In [26,36] it was observed that high-power super-Gaussian (flat-top) initial conditions collapse with a ring profile. In [41], Grow et al. used a geometrical optics argument to explain why high-power super-Gaussian initial conditions always collapse with a ring profile. Although only solutions of the critical NLS were discussed in [41], the geometrical optics argument is also valid for the supercritical NLS. To see this numerically, in Fig. 25 we solve the supercritical NLS (55) for $d = 2.1$ and $\sigma = 1.1$ ($\alpha \approx 0.7438$) with the super-Gaussian initial condition $\psi_0(r) = 15e^{-r^4}$. As expected, the solution evolves into a ring-like shape after very little focusing (Fig. 25B). As the solution continues to collapse the ring-like profile converges to the ψ_Q profile (Fig. 25D).

8. Stability of supercritical ring solutions — numerical simulations

We have already tested numerically the stability of singular ring solutions for the case $\alpha = 0$, see Figs. 13 and 14, and for the case $\alpha = 1$, see Fig. 6 and [26]. In all these cases, the ring solutions were stable with respect to radially symmetrical perturbations, but unstable with respect to symmetry breaking simulations.

We now show that the same also holds for $0 < \alpha < 1$. For example, in Fig. 26 we randomly perturb the initial ring profile from Fig. 18 ($\sigma = 1.1$, $d = 2.1$, $\alpha \approx 0.74380$) as in (52). After focusing by less than two, the noise in ring region (i.e. the area of high nonlinearity) disappears (Fig. 26B). Subsequently, the noise at the inner and outer regions slowly decreases, until after focusing by a factor of 50, the solution approaches a clean ring profile. Similar results were obtained $d = 3$ and $\sigma = 1.5$ ($\alpha = 1/8$), data not shown. We, therefore, conclude that the self-similar ring profile ψ_Q is a strong attractor as a solution of the radially-symmetrical NLS (55) for all α such that $0 \leq \alpha \leq 1$.

We now test the stability of the supercritical ring profile with respect to symmetry breaking perturbations. As noted, this test can only be conducted for integer values of d . To do so, we solve the two-dimensional NLS

$$i\psi_t(t, x, y) + \psi_{xx} + \psi_{yy} + |\psi|^{2\sigma}\psi = 0, \quad (87)$$

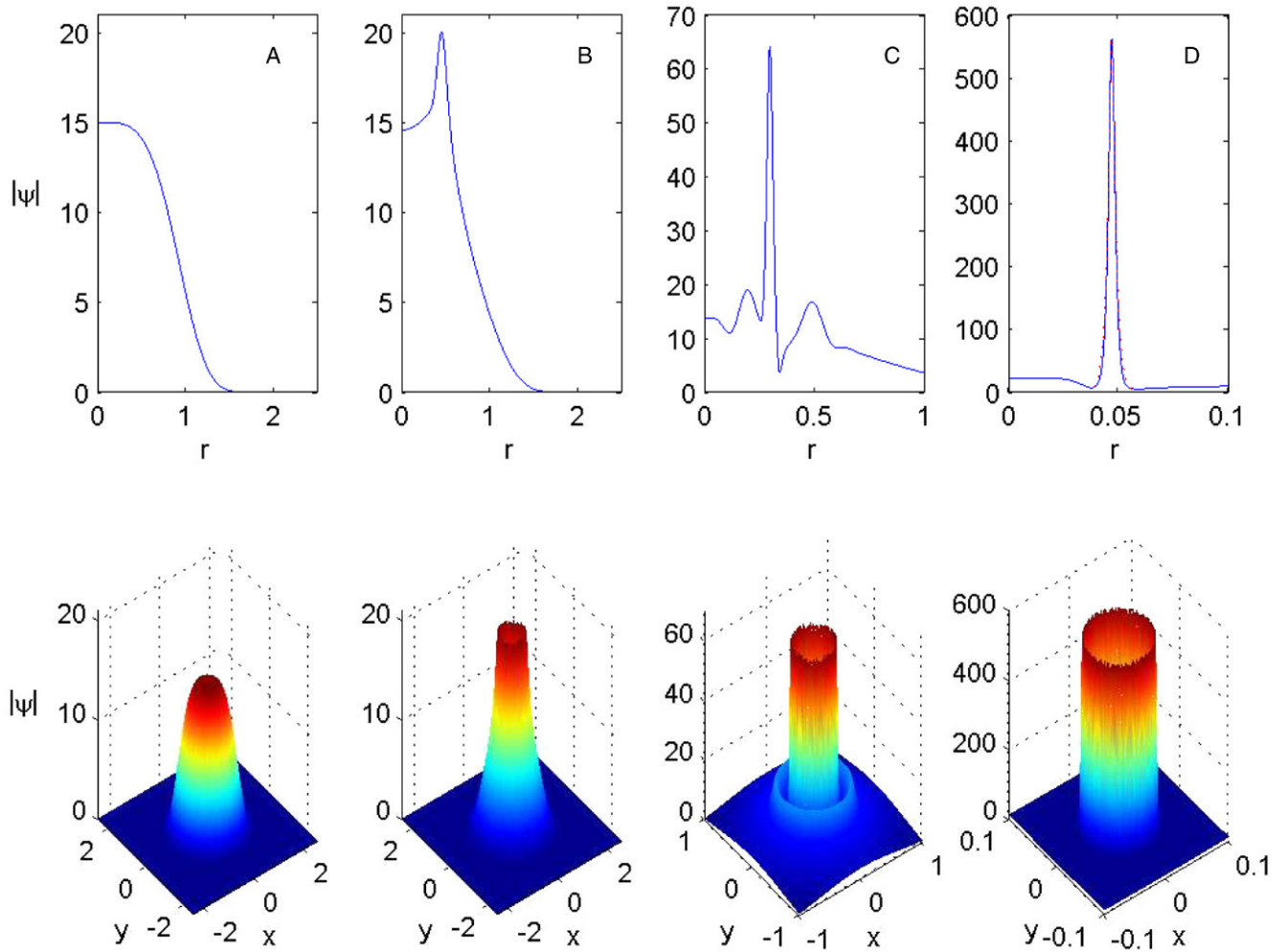


Fig. 25. Top: Solution of supercritical NLS (55) for $d = 2.1$ and $\sigma = 1.1$ with super-Gaussian initial condition $\psi_0 = 15e^{-r^4}$. A: $t = 0$, ($1/L = 1$); B: $t = 0.011$, ($1/L = 1.33$); C: $t = 0.017$, ($1/L = 4.27$); D: $t = 0.013$, ($1/L = 37.42$). Dotted curve in D is $|\psi_Q|$, both curves are indistinguishable around the peak. Bottom: Same data as in top graphs, plotted as two-dimensional surfaces.

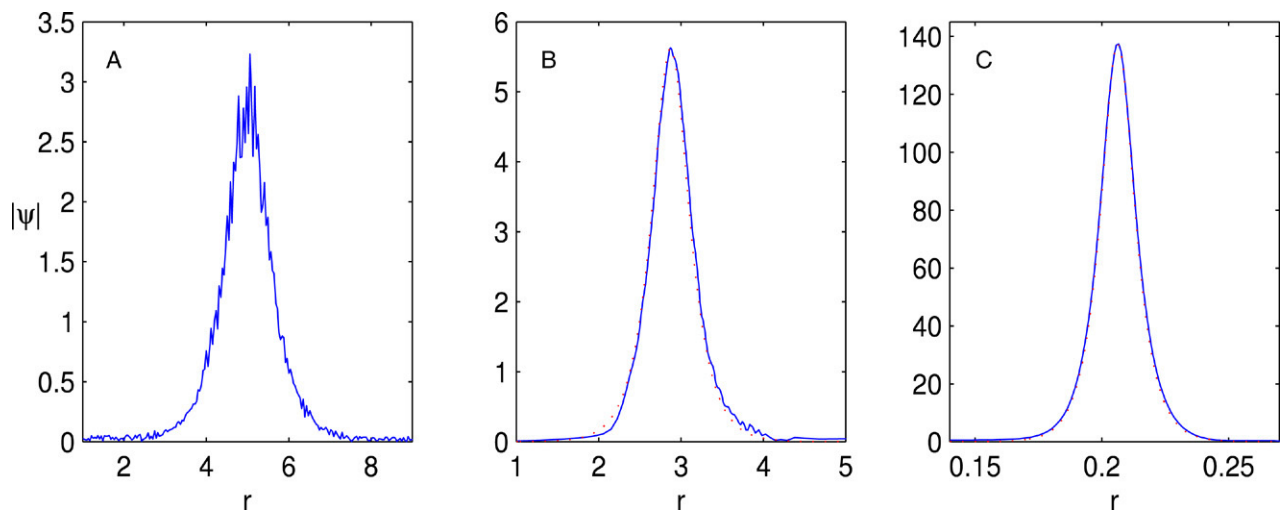


Fig. 26. Solution of the NLS (55) with $d = 2.1$, $\sigma = 1.1$ ($\alpha \approx 0.74380$) and with the noisy initial condition (52). A: $t = 0$, ($1/L = 1$); B: $t = 0.14$, ($1/L = 2$); C: $t = 0.26$, ($1/L = 71.73$). Dotted curve in B and C is the ψ_Q profile, where Q is given by (77).

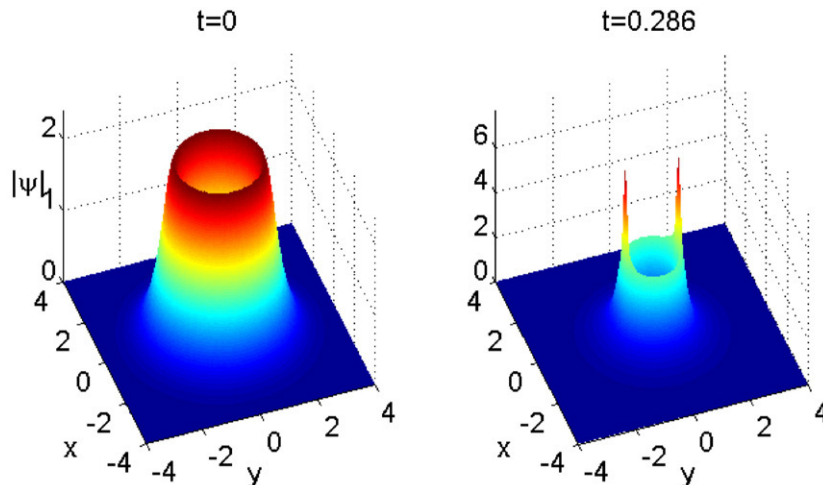


Fig. 27. Solution of the NLS (87) for $\sigma = 1.5$ with slightly elliptical initial condition (88).

with $\sigma = 1.5$ ($\alpha = 1/3$), with the slightly elliptical initial condition

$$\psi_Q^{0,\text{elliptic}} = \psi_Q^0(\sqrt{1.02x^2 + y^2}), \quad (88)$$

where ψ_Q^0 is given by (84).

After very little focusing, two filaments emerge on the intersection of the ring with the y -axis (see Fig. 27). Therefore, the collapsing ring solution is unstable as a solution of the NLS (87), i.e. with respect to perturbations that breakup the radial symmetry.

9. Supercritical rings in the case $\sigma > 2$ — preliminary numerical investigation

In Sections 3–6 we study supercritical ring solutions for $2/d \leq \sigma \leq 2$. We now briefly consider the case $\sigma > 2$. In this case, the ring profile ψ_Q , see Eq. (63), fails to describe ring solutions. Indeed, according to relation (72), $\alpha < 0$ for $\sigma > 2$, whereas the admissible values of α are $0 \leq \alpha \leq 1$ (Lemma 8). Therefore, it is natural to ask whether singular ring solutions exist for $\sigma > 2$. To answer this question, we solve the supercritical NLS (55) for the case of $\sigma = 2.1$ and $d = 2$ with the ring initial condition (49). Note that unlike the simulations of Section 6, we could not use the initial condition (84) since $\alpha < 0$. In Fig. 28, we plot the early stages of the collapse as the solution focuses by a factor of ≈ 3 . The solution seems to undergo a standing ring collapse, i.e. as the amplitude increases, the ring radius does not go to zero, but rather converges to a positive value. In Fig. 29 we plot the solution as it continues to collapse by 10 orders of magnitude and observe that the solution continues to collapse as a standing ring solution (Fig. 29A). As in the case $\sigma \leq 2$, the solution collapses with a self-similar ring profile. However, the self-similar profile does not match the Q profile (77), see Fig. 29B. Fig. 29C and D suggest that the blowup rate is a square root, with no loglog correction.

Additional simulations for $d = 2$ and $\sigma = 2.2, 2.3, 2.4$, as well as for $d = 1.1$ and $\sigma = 2.1$ (data not shown) yielded the

same qualitative results. Therefore, our preliminary simulations suggest that there exist collapsing ring solutions in the case $\sigma > 2$, and that these solutions have the following properties:

- (1) Standing-ring collapse, i.e. the ring's radius approaches a positive constant as the solution collapses.
- (2) The collapsing part of the solution has an asymptotic self-similar ring profile

$$|\psi| \sim \frac{1}{L^{1/\sigma}(t)} F\left(\frac{r - r_m(t)}{L(t)}\right).$$

- (3) The asymptotic profile F is different from the Q profile (77).
- (4) The blowup rate is a square root with no loglog correction.

These observations suggest that $\sigma = 2$ is a *critical exponent* of the supercritical NLS, in a sense that ring solutions behave differently for the case $\sigma < 2$, $\sigma = 2$ and $\sigma > 2$. A systematic study of the regime $\sigma > 2$ will be presented elsewhere.

10. Numerical methods

10.1. Simulations of the NLS (Iterative grid redistribution)

Since the 1980s, a highly successful method for a simulations of collapsing (equal-rate) solutions of the NLS has been the method of *dynamic rescaling* [9,24]. In this method, the independent variables and the function are dynamically rescaled in a way which is based on the asymptotic form (56), i.e.

$$\psi(t, r) = \frac{1}{L^{1/\sigma}(t)} \phi(\tau, \rho), \quad \tau = \int_0^t \frac{ds}{L^2(s)}, \quad \rho = \frac{r}{L}. \quad (89)$$

As a result, $\phi(\tau, \rho)$ remains smooth as $L \rightarrow 0$, and the rescaled problem for ϕ can be solved on a fixed grid (in ρ) using standard techniques.

The dynamic rescaling method works only for equal-rate collapsing solutions, since it is based on the asymptotic form (56). In particular, the dynamic rescaling method cannot be used for simulations of standing rings, since they do not

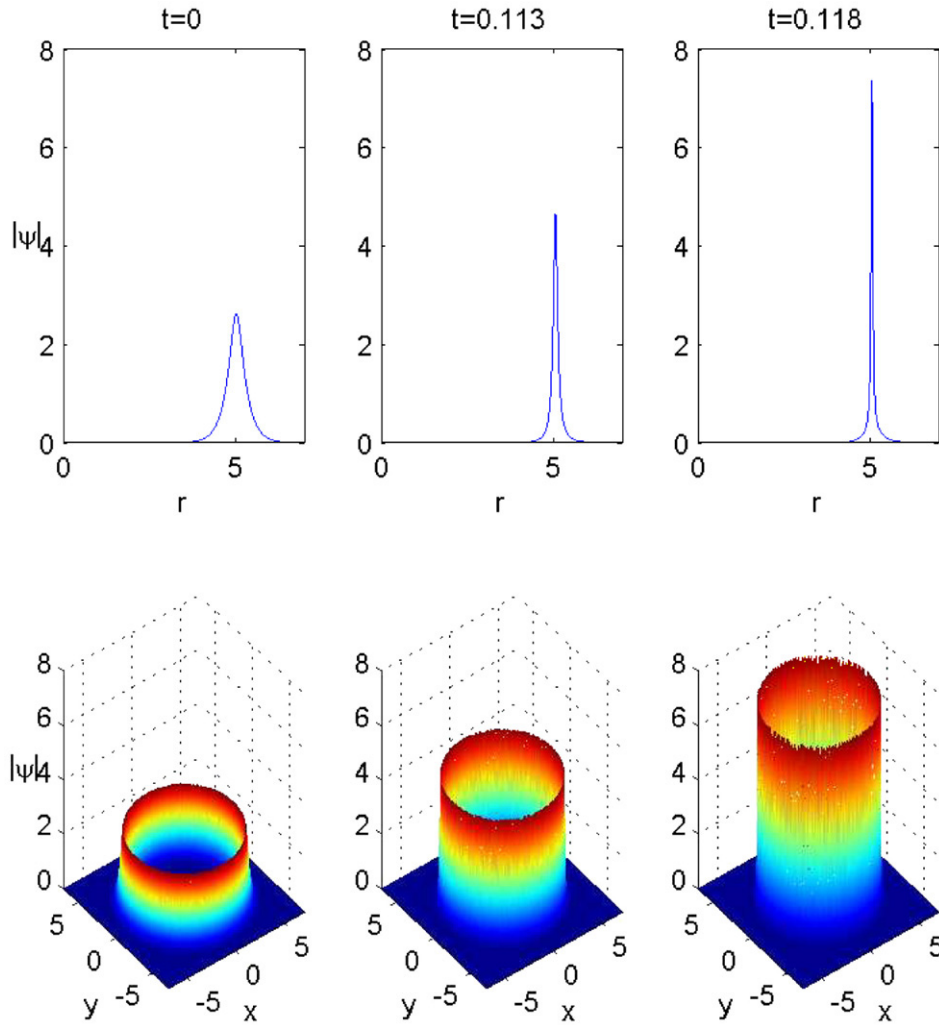


Fig. 28. Solution of the NLS (55) with $\sigma = 2.1$ and $d = 2$ with ψ_0 given by (49).

become singular at the origin. The dynamic rescaling method also fails for singular rings solutions that collapse towards the origin in the case $0 < \alpha < 1$, since these solutions do not undergo equal-rate collapse. In addition, since the dynamic rescaling method contracts grid points toward the singularity, it fails when the simulation includes multiple regions of singular behaviour, such as in multiple filamentation (e.g. see Figs. 14 and 27).

To overcome these limitations of the dynamics rescaling method we used the iterative grid redistribution (IGR) method for the simulations of the NLS with and without radial symmetry. The IGR method was introduced by Ren and Wang in [42] and further improved in [43,44]. As with dynamic rescaling, this method allows the grid points to move towards regions of steep gradients such that the solution remains smooth in the transformed grid. For example, although the solution in Fig. 30A is very close to singular, it is smooth in the computational grid, see Fig. 30B. After the grid is remeshed, i.e. the grid points are moved, the problem is solved on a fixed grid using standard techniques until the solution becomes nonsmooth again and grid is remeshed again. Unlike

dynamic rescaling, the grid points are not uniformly remeshed according to a known asymptotic profile. Instead, the grid points remeshing is determined from a variational principle that makes no assumptions on the asymptotic profile of the solution. For details, see [42–44].

10.2. Recovering L and L_t from the simulation result

In general, the numerical values of L and LL_t are different from the value used in the asymptotic theory. This is because numerically the expected phase is of the form

$$S = i\lambda\tau + i\alpha \frac{L_t}{4L} r^2 + i(1 - \alpha) \frac{L_t}{4L} (r - r_0 L^\alpha)^2,$$

while in the asymptotic theory we arbitrary set $\lambda = 1$. The variables L and L_t can be recovered using [45]

$$L = \frac{Q(0)}{\psi(\rho = 0)} \bar{L}, \quad LL_t = \frac{Q^2(0)}{\psi^2(\rho = 0)} \bar{L} \bar{L}_t, \quad (90)$$

where the bars denote the measured value of L and L_t .

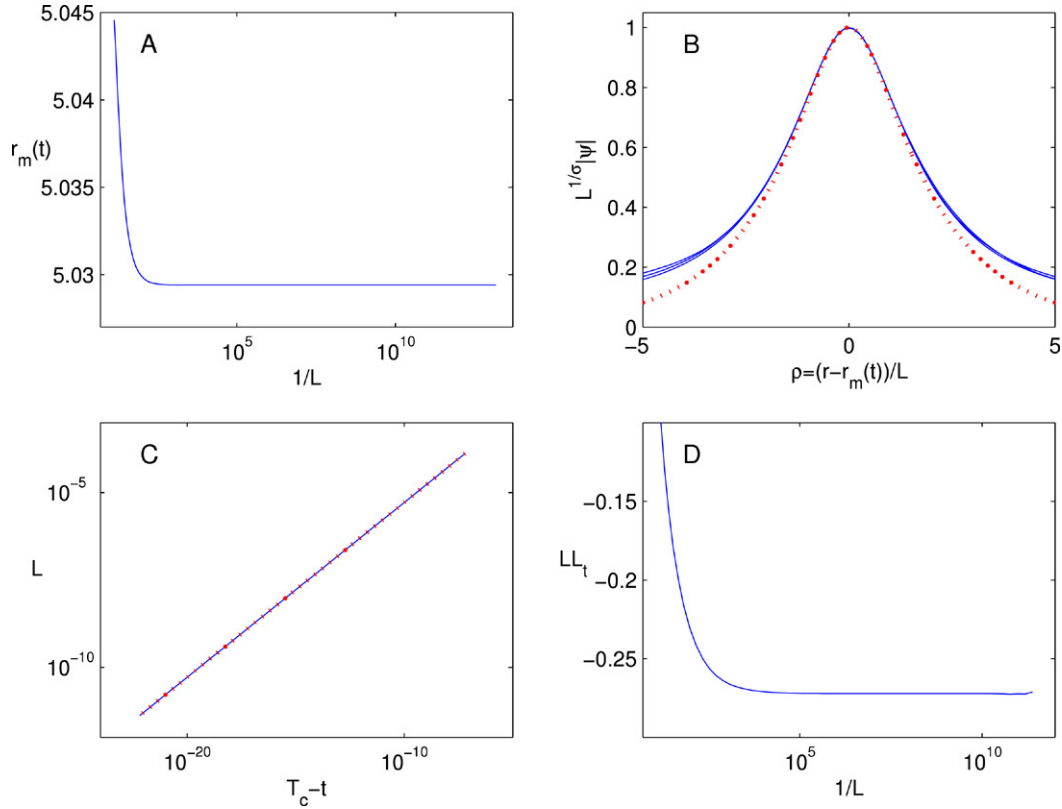


Fig. 29. Solution of Fig. 28. A: $r_m(t)$ as a function of L . B: Rescaled solution according to (51) at focusing levels $1/L = 271.07$ (solid), $1/L = 2.21 \times 10^6$ (dashed) and $1/L = 1.84 \times 10^{12}$ (dash-dots), all three curves are indistinguishable. Dotted curve is the asymptotic profile (77). C: L as a function of $(T_c - t)$. Dotted curve is the fitted curve $L \sim c(T_c - t)^{0.49996}$ where $c = 0.5209$. D: LL_t as a function of $1/L$.

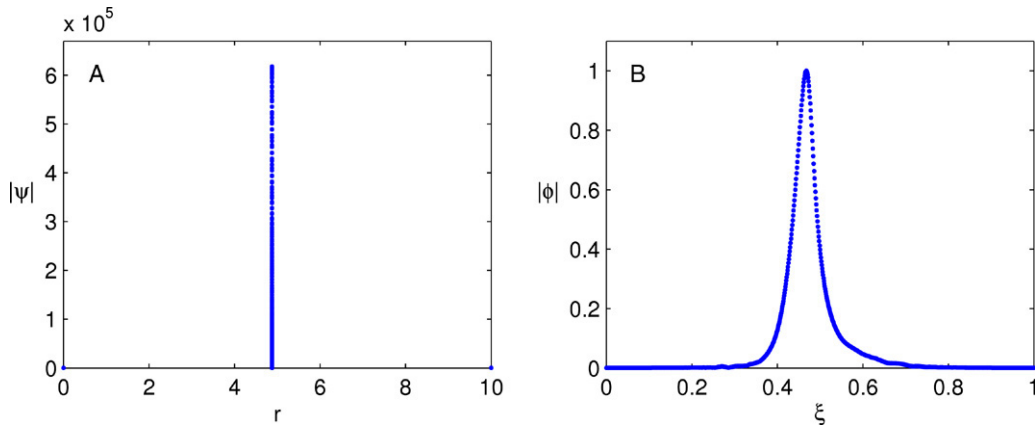


Fig. 30. Solution of Fig. 7 at $L^{-1} = 3.8 \times 10^{11}$. A: Physical grid. B: Computational grid.

10.3. Validation of the filamentation pattern in Figs. 14 and 27

Since the NLS (1) is isotropic, the symmetry breaking induced by ellipticity of the initial condition, see e.g. Eq. (88), preserves the symmetries $x \rightarrow -x$ and $y \rightarrow -y$. Therefore, the filamentation pattern induced by ellipticity should preserve these two symmetries [46] as is, indeed, the case in Figs. 14 and 27. However, we still need to verify that these filamentation patterns are due to the small ellipticity of the initial condition and not a numerical artifact caused by the preferred directions of the numerical Cartesian grid. To do so, we repeated the simulation with the same initial condition after it was rotated

by 30° . In this case, the two filaments are rotated by an angle of $\approx 30^\circ$, see Fig. 31B. Therefore, we conclude that the multiple filamentation is indeed due to the small ellipticity of the initial condition.

Appendix A. Definition of the blowup

In this study, we use the following definition for the blowup rate:

$$L(t) = \frac{\|\psi(0, \cdot)\|_\infty^\sigma}{\|\psi(t, \cdot)\|_\infty^\sigma}, \quad (\text{A.1})$$

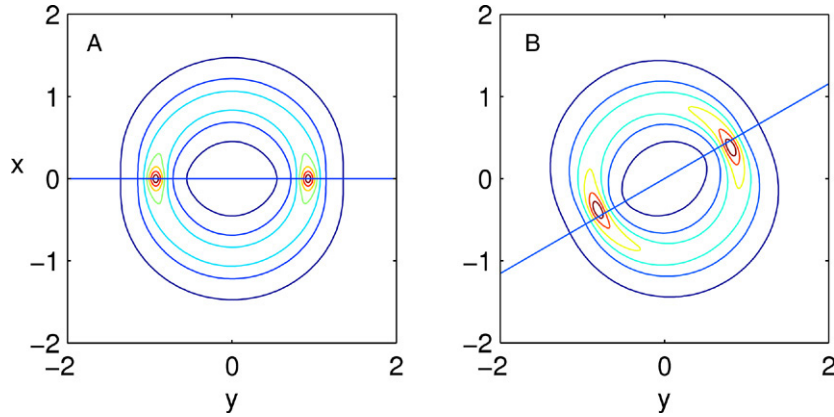


Fig. 31. A: Level sets of the solution of Fig. 27 at $t = 0.286$; solid curve is the y -axis. B: Same as A, with the initial condition rotated by 30° ; solid curve is 30° from the y -axis.

which is based on Eq. (21a). The common definition of the blowup rate in NLS theory is, however,

$$L_{\text{def}}(t) = \|\nabla\psi\|_2^{-1}. \tag{A.2}$$

It is well known that (A.1) and (A.2) are equivalent, up to a multiplicative constant, for solutions that collapse with the standard asymptotic form (56), such as the ψ_R profile (8) and the critical ring solutions ψ_G that undergo equal-rate collapse ($\alpha = 1$).

The following lemma shows that (A.1) and (A.2) are also equivalent for supercritical solutions that collapse with the new ring asymptotic profile (63):

Lemma 25. *Let ψ be a singular ring solution of the NLS (55) with an asymptotic blowup profile $\psi(t, r) \sim \psi_Q(t, r)$, where ψ_Q is given by (63). Let $0 \leq \alpha \leq 1$. Then (A.1) and (A.2) are equivalent, i.e., $L_{\text{def}}(t) \sim cL(t)$ as $t \rightarrow T_c$, where c is a constant.*

Proof. The case $\alpha = 1$ is well known. We first prove the lemma for $\alpha = 0$. In this case

$$\begin{aligned} \|\nabla\psi_Q\|_2^2 &= \int_{r=0}^{\infty} \left| \frac{\partial}{\partial r} \psi'_Q \right|^2 r^{d-1} dr \\ &= L^{-1-\frac{2}{\sigma}} \int_{\rho=-r_0L^{-1}}^{\infty} \left[\left(\frac{\partial}{\partial \rho} Q \right)^2 + \frac{(LL_t)^2}{4} Q^2 \rho^2 \right] \\ &\quad \times (L\rho + r_0)^{d-1} d\rho. \end{aligned}$$

By Lemma 12, $\sigma = 2$ hence $-1 - \frac{2}{\sigma} = -2$. In addition, since L is faster than or equal to a square root, i.e.

$$L \sim f_c \sqrt{T_c - t}, \quad f_c \geq 0,$$

then $LL_t \rightarrow -\frac{f_c^2}{2}$. Therefore, as $t \rightarrow T_c$,

$$\begin{aligned} \int_{r=0}^{\infty} |\psi'_Q|^2 r^{d-1} dr \\ = L^{-2} \int_{\rho=-\infty}^{\infty} \left[(Q')^2 + \frac{f_c^4}{16} Q^2 \rho^2 \right] r_0^{d-1} d\rho. \end{aligned}$$

Hence

$$L_{\text{def}}(t) = c \cdot L(t),$$

$$c = \left[r_0^{d-1} \int_{\rho=-\infty}^{\infty} (Q')^2 + \frac{f_c^4}{16} Q^2 \rho^2 d\rho \right]^{-\frac{1}{2}}.$$

For $0 < \alpha < 1$,

$$\begin{aligned} \|\nabla\psi_Q\|_2^2 &= L^{-1-\frac{2}{\sigma}} \int_{\rho=-r_0L^{\alpha-1}}^{\infty} \left[(Q'(\rho))^2 \right. \\ &\quad \left. + \left(\frac{2\alpha(L\rho + r_0L^\alpha) + 2(1-\alpha)L\rho}{16} \right)^2 L_t^2 Q^2(\rho) \right] \\ &\quad \times (L\rho + r_0L^\alpha)^{d-1} d\rho. \end{aligned}$$

Since $\alpha < 1$, as $L \rightarrow 0$,

$$\begin{aligned} \|\nabla\psi_Q\|_2^2 &= L^{\alpha(d-1)-1-\frac{2}{\sigma}} \\ &\quad \times \int_{\rho=-\infty}^{\infty} \left[(Q'(\rho))^2 + \frac{4\alpha r_0^2 (L^\alpha L_t)^2}{16} Q^2(\rho) \right] r_0^{d-1} d\rho. \end{aligned}$$

By Lemma 20, $\alpha(d-1) - 1 - \frac{2}{\sigma} = -2$, and L is faster than or equal to $(T_c - t)^{\frac{1}{1+\alpha}}$, i.e.

$$L \sim f_c (T_c - t)^{\frac{1}{1+\alpha}}, \quad f_c \geq 0.$$

Hence, $L^\alpha L_t = -\frac{f_c^{1+\alpha}}{1+\alpha}$. Therefore, as $t \rightarrow T_c$,

$$\begin{aligned} \|\nabla\psi_Q\|_2^2 &\approx \frac{1}{L^2} r_0^{d-1} \\ &\quad \times \int_{-\infty}^{\infty} \left((Q'(\rho))^2 + \frac{\alpha^2 r_0^2 f_c^{2(1+\alpha)}}{4(1+\alpha)^2} Q^2(\rho) \right) d\rho. \end{aligned}$$

Hence

$$\begin{aligned} L_{\text{def}}(t) &= c \cdot L(t), \quad c = \left[r_0^{d-1} \int_{-\infty}^{\infty} \left((Q'(\rho))^2 \right. \right. \\ &\quad \left. \left. + \frac{\alpha^2 r_0^2 f_c^{2(1+\alpha)}}{4(1+\alpha)^2} Q^2(\rho) \right) d\rho \right]^{-\frac{1}{2}}. \end{aligned}$$

Appendix B. Proof of Lemma 9

The boundary condition $Q(\infty) = 0$ follows from the requirement that Q has a finite power (L^2 norm). Since $\psi_Q(r)$, as defined by (63) is radially symmetric in r , then $\frac{d}{d\rho}Q(\rho)|_{r=0} = 0$. For $\alpha = 1$, $r = 0$ corresponds to $\rho = -r_0$, see (63b). Therefore, in this case, the left boundary condition is $\frac{d}{d\rho}Q(-r_0) = 0$. Otherwise, for $0 \leq \alpha < 1$, $r = 0$ corresponds to $\rho = -\frac{r_0}{L^{1-\alpha}}$. Therefore, when $L \rightarrow 0$, the left boundary is at $\rho = -\infty$ and the left boundary condition is $\frac{d}{d\rho}Q(-\infty) = 0$.

Appendix C. Nonexistence of ring solutions to the R equation

We define ring solutions as radial solutions whose global maximum is attained at some $r > 0$, in contrast with peak solutions whose global maximum is attained at $r = 0$.

Lemma 26. *The equation*

$$R''(r) + \frac{d-1}{r}R' - R + R^{2\sigma+1} = 0, \quad (C.1)$$

$$R'(0) = 0 \quad 2/d \leq \sigma, 1 < d,$$

does not admit H^1 ring solutions.

Proof. If $R \in H^1$ then $\lim_{r \rightarrow \infty} R(r) = 0$ and either $\lim_{r \rightarrow \infty} R'(r) = 0$ or $R'(r)$ does not have a limit as $r \rightarrow \infty$.

To show that $\lim_{r \rightarrow \infty} R'(r) = 0$, let us define

$$N(r) = (R'(r))^2 - R^2 + \frac{1}{1+\sigma}R^{2+2\sigma}.$$

Since

$$N(r) - N(0) = -2(d-1) \int_0^r \frac{1}{s} (R'(s))^2 ds,$$

then $N(r)$ is monotonically decreasing in r . This implies that $N(r)$ has a limit, i.e.

$$\lim_{r \rightarrow \infty} N(r) = N_\infty, \quad -\infty \leq N_\infty < \infty.$$

In addition, since $\lim_{r \rightarrow \infty} R(r) = 0$, then

$$N_\infty = \lim_{r \rightarrow \infty} N(r) = \lim_{r \rightarrow \infty} (R'(r))^2 \geq 0.$$

Hence, N_∞ is finite and therefore $\lim_{r \rightarrow \infty} R'(r) = 0$.

Since $\lim_{r \rightarrow \infty} R'(r) = 0$, then $N_\infty = 0$. Therefore, $N(r) > 0$ for any $0 \leq r < \infty$. Hence, if $R'(r) = 0$ then $R(r) > R_c$, where $R_c = \sqrt[2\sigma]{\sigma + 1}$.

Let us now assume that there exists a maxima point at $r_m > 0$. Since $R'(0) = R'(r_m) = 0$, then, by the previous argument, both $R(0)$ and $R(r_m)$ are above R_c . In addition, since $N(r)$ is monotonically decreasing in r , then $N(0) > N(r_m)$. Since

$$N = (R')^2 + R^2 \left(\left(\frac{R}{R_c} \right)^{2\sigma} - 1 \right),$$

then, for $R > R_c$, $N(R, R')$ is monotonically increasing in R along the line $R' = 0$. Therefore,

$$N(R(0), R' = 0) = N(r = 0) > N(r = r_m) \\ = N(R(r_m), R' = 0)$$

implies that $R(0) > R(r_m)$.

Appendix D. Proof of Lemma 10

When $\varepsilon = 0$, the solution of Eq. (65) can be explicitly calculated and is given by

$$Q = (1 + \sigma)^{\frac{1}{2\sigma}} \operatorname{sech}^{\frac{1}{\sigma}}(\sigma\rho).$$

Assume that a solution to Eq. (65) exists for $\varepsilon \neq 0$. Let $u = Q + \varepsilon u_1 + \mathcal{O}(\varepsilon^2)$. The equation for u_1 is

$$u_1''(\rho) - u_1 + (\sigma + 1)Q^{2\sigma}u_1 + \sigma Q^{2\sigma}u_1^* = (a + bi)Q + c\rho Q'.$$

Let $u_1 = S + iT$ where $S = \operatorname{Re}(u_1)$ and $T = \operatorname{Im}(u_1)$. Then the equations for S and T are

$$S''(\rho) - S + (2\sigma + 1)Q^{2\sigma}S = (\operatorname{RHS})_S, \\ T''(\rho) - T + Q^{2\sigma}T = (\operatorname{RHS})_T,$$

where

$$(\operatorname{RHS})_S = aQ + c\rho Q', \quad (\operatorname{RHS})_T = bQ.$$

The solvability condition for S is $\int_{-\infty}^{\infty} (\operatorname{RHS})_S Q' d\rho = 0$, and for T is $\int_{-\infty}^{\infty} (\operatorname{RHS})_T Q d\rho = 0$, see [47]. Since Q is an even function, $(\operatorname{RHS})_S Q'$ is an odd function, hence $\int_{-\infty}^{\infty} (\operatorname{RHS})_S Q' d\rho = 0$. Therefore, the equation for S is solvable. The equation for T , however, is solvable only if $b = 0$, since

$$\int_{-\infty}^{\infty} (\operatorname{RHS})_T Q d\rho = b \int_{-\infty}^{\infty} Q^2 d\rho.$$

Appendix E. Proof of Lemma 24

We first show that when $\alpha = 1$, the singular ring solutions undergo strong collapse. Indeed, in this case,

$$P_\varepsilon = \lim_{t \rightarrow T_c} \int_{0 \leq r < \varepsilon} |\psi_Q|^2 r^{d-1} dr \\ = \lim_{t \rightarrow T_c} \int_{0 \leq r < \varepsilon} \frac{1}{L^{2/\sigma}} Q^2 \left(\frac{r - r_0 L}{L} \right) r^{d-1} dr \\ = \lim_{t \rightarrow T_c} \int_{0 \leq L\rho + r_0 L < \varepsilon} \frac{1}{L^{2/\sigma}} Q^2(\rho) (L\rho + r_0 L)^{d-1} (L d\rho) \\ = L^{(d-1)+1-2/\sigma} \lim_{t \rightarrow T_c} \int_{0 \leq L\rho + r_0 L < \varepsilon} Q^2(\rho) (\rho + r_0)^{d-1} d\rho.$$

Lemma 18 implies that if $\alpha = 1$ then $\sigma d = 2$. Hence

$$P_\varepsilon = \lim_{t \rightarrow T_c} \int_{0 \leq L\rho + r_0 L < \varepsilon} Q^2(\rho) (\rho + r_0)^{d-1} d\rho \\ = \lim_{t \rightarrow T_c} \int_{-r_0 \leq \rho < \varepsilon/L - r_0} Q^2(\rho) (\rho + r_0)^{d-1} d\rho \\ = \int_{-r_0 \leq \rho < \infty} Q^2(\rho) (\rho + r_0)^{d-1} d\rho = \|\psi_Q^0\|_2^2.$$

Hence

$$P_{\text{collapse}} = \inf_{\varepsilon} P_{\varepsilon} = \|\psi_Q^0\|_2^2.$$

We now show that when $0 < \alpha < 1$ the new singular ring solutions also undergo strong collapse. Indeed

$$\begin{aligned} P_{\varepsilon} &= \lim_{t \rightarrow T_c} \int_{0 \leq r < \varepsilon} |\psi_Q|^2 r^{d-1} dr \\ &= \lim_{t \rightarrow T_c} \int_{0 \leq r < \varepsilon} \frac{1}{L^{2/\sigma}} Q^2 \left(\frac{r - r_0 L^{\alpha}}{L} \right) r^{d-1} dr \\ &= \lim_{t \rightarrow T_c} \int_{0 \leq L\rho + r_0 L^{\alpha} < \varepsilon} \frac{1}{L^{2/\sigma}} Q^2(\rho) (L\rho + r_0 L^{\alpha})^{d-1} (L d\rho). \end{aligned}$$

Since $0 < \alpha < 1$ and $\lim_{t \rightarrow T_c} L(t) = 0$,

$$(L\rho + r_0 L^{\alpha})^{d-1} \approx r_0^{d-1} L^{\alpha(d-1)}, \quad t \rightarrow T_c.$$

Hence, using relation (72),

$$\begin{aligned} P_{\varepsilon} &= r_0^{d-1} \lim_{t \rightarrow T_c} \int_{\rho = -r_0 L^{\alpha-1}}^{\frac{1}{L}(\varepsilon - r_0 L^{\alpha})} Q^2(\rho) L^{\alpha(d-1)+1-2/\sigma} d\rho \\ &= r_0^{d-1} \int_{-\infty}^{\infty} Q^2 d\rho. \end{aligned}$$

Therefore,

$$P_{\text{collapse}} = \inf_{\varepsilon} P_{\varepsilon} = r_0^{d-1} \int_{-\infty}^{\infty} Q^2 d\rho. \quad (\text{E.1})$$

Appendix F. Admissible values of α — power conservation violation for $\alpha < 0$

Let us assume that ψ_Q exists. Then the power of ψ_Q is

$$\begin{aligned} \int |\psi_Q|^2 &= L^{-2/\sigma} \int_0^{\infty} Q^2 \left(\frac{r - r_0 L^{\alpha}}{L} \right) r^{d-1} dr \\ &\approx L^{-2/\sigma} \int_{-\infty}^{\infty} Q^2(\rho) (L\rho + r_0 L^{\alpha})^{d-1} (L d\rho) \\ &\approx L^{\alpha(d-1) + \frac{\sigma-2}{\sigma}} \int_{-\infty}^{\infty} Q^2(\rho) d\rho. \end{aligned}$$

Since $\sigma \leq 2$, $1 < d$ and $\alpha < 0$, then

$$\alpha(d-1) + \frac{\sigma-2}{\sigma} < 0.$$

Therefore,

$$\lim_{L \rightarrow 0} \int |\psi_Q|^2 = \infty,$$

which is in contradiction with power conservation.

References

[1] G. Fibich, G. Papanicolaou, Self-focusing in the perturbed and unperturbed nonlinear Schrödinger equation in critical dimension, *SIAM J. Appl. Math.* 60 (1999) 183–240.
 [2] W. Strauss, *Nonlinear Wave Equations*, American Mathematical Society, Providence, RI, 1989.
 [3] C. Sulem, P. Sulem, *The Nonlinear Schrödinger Equation*, Springer, New-York, 1999.

[4] M. Grillakis, Existence of nodal solutions of semilinear equations in \mathbb{R}^N , *J. Differential Equations* 85 (1990) 367–400.
 [5] R. Chiao, E. Garmire, C. Townes, Self-trapping of optical beams, *Phys. Rev. Lett.* 13 (1964) 479–482.
 [6] M. Weinstein, Nonlinear Schrödinger equations and sharp interpolation estimates, *Comm. Math. Phys.* 87 (1983) 567–576.
 [7] V. Talanov, Focusing of light in cubic media, *JETP Lett.* 11 (1970) 199–201.
 [8] M. Landman, G. Papanicolaou, C. Sulem, P. Sulem, X. Wang, Stability of isotropic singularities for the nonlinear Schrödinger equation, *Physica D* 47 (1991) 393–415.
 [9] D. McLaughlin, G. Papanicolaou, C. Sulem, P. Sulem, Focusing singularity of the cubic Schrödinger equation, *Phys. Rev. A* 34 (1986) 1200–1210.
 [10] G. Frیمان, Asymptotic stability of manifold of self-similar solutions in self-focusing, *Sov. Phys. JETP* 61 (1985) 228–233.
 [11] M. Landman, G. Papanicolaou, C. Sulem, P. Sulem, Rate of blowup for solutions of the nonlinear Schrödinger equation at critical dimension, *Phys. Rev. A* 38 (1988) 3837–3843.
 [12] B. LeMesurier, G. Papanicolaou, C. Sulem, P. Sulem, Local structure of the self-focusing singularity of the nonlinear Schrödinger equation, *Physica D* 32 (1988) 210–226.
 [13] B. LeMesurier, G. Papanicolaou, C. Sulem, P. Sulem, Focusing and multi-focusing solutions of the nonlinear Schrödinger equation, *Physica D* 31 (1988) 78–102.
 [14] M. Weinstein, The nonlinear Schrödinger equation — singularity formation, stability and dispersion, *Contemp. Math.* 99 (1989) 213–232.
 [15] H. Nawa, Asymptotic profiles of blow-up solutions of the nonlinear Schrödinger equation with critical power nonlinearity, *J. Math. Soc. Japan* 46 (1994) 557–586.
 [16] H. Nawa, Asymptotic and limiting profiles of blow-up solutions of the nonlinear Schrödinger equation with critical power, *Comm. Pure Appl. Math.* 52 (1999) 193–270.
 [17] F. Merle, P. Raphael, Sharp upper bound on the blow-up rate for the critical nonlinear Schrödinger equation, *Geom. Funct. Anal.* 13 (2003) 591–642.
 [18] F. Merle, P. Raphael, On universality of blow-up profile for L^2 critical nonlinear Schrödinger equation, *Invent. Math.* 156 (2004) 565–672.
 [19] F. Merle, P. Raphael, Profiles and quantization of the blow up mass for critical nonlinear Schrödinger equation, *Comm. Math. Phys.* 253 (2005) 675–704.
 [20] F. Merle, P. Raphael, On a sharp lower bound on the blow-up rate for the critical nonlinear Schrödinger equation, *J. Amer. Math. Soc.* 19 (2006) 37–90.
 [21] K. Moll, A. Gaeta, G. Fibich, Self-similar optical wave collapse: Observation of the Townes profile, *Phys. Rev. Lett.* 90 (2003) 203902.
 [22] B. LeMesurier, G. Papanicolaou, C. Sulem, P. Sulem, The focusing singularity of the nonlinear Schrödinger equation, in: M. Grandall, P. Rabinovitz, R. Turner (Eds.), *Directions in Partial Differential Equations*, Academic Press, New-York, 1987, pp. 159–201.
 [23] N. Kosmatov, I. Petrov, V. Shvets, V. Zakharov, Large scale amplitude simulation of wave collapse in nonlinear Schrödinger equations, *Academy of Sciences of the USSR, Space Research Institute*. Preprint.
 [24] N. Kosmatov, V. Shvets, V. Zakharov, Computer simulation of wave collapses in the nonlinear Schrödinger equation, *Physica D* 52 (1991) 16–35.
 [25] C.J. Budd, Asymptotics of multibump blow-up self-similar solutions of the nonlinear Schrödinger equation, *SIAM J. Appl. Math.* 62 (2001) 801–830.
 [26] G. Fibich, N. Gavish, X. Wang, New singular solutions of the nonlinear Schrödinger equation, *Physica D* 211 (2005) 193–220.
 [27] P. Raphael, Existence and stability of a solution blowing up on a sphere for a L^2 supercritical non linear Schrödinger equation, *Duke Math. J.* 134 (2) (2006) 199–258.
 [28] F. Merle, Construction of solutions with exactly k blow-up points for the Schrödinger equation with the critical power nonlinearity, *Comm. Math. Phys.* 129 (1990) 223–240.

- [29] L. Degtiarev, V.E. Zakharov, L.I. Rudakov, Two examples of langmuir wave collapse, *JETP* 41 (1) (1975) 57–61.
- [30] T. Cazenave, F. Weissler, The Cauchy problem for the critical nonlinear Schrödinger equation in H^s , *Nonlinear Anal.* 14 (1990) 807–836.
- [31] F. Merle, Limit of the solution of a nonlinear Schrödinger equation at blow-up time, *J. Funct. Anal.* 84 (1989) 201–214.
- [32] T. Cazenave, F. Weissler, The Cauchy problem for the nonlinear Schrödinger equation in H^1 , *Manuscripta Math.* 61 (1988) 477–498.
- [33] F. Merle, Lower bounds for the blow-up rate of solutions of the Zakharov equation in dimension two, *Comm. Pure Appl. Math.* 49 (1996) 765–794.
- [34] G. Perelman, On the formation of singularities in solutions of the critical nonlinear Schrödinger equation, *Ann. Henri Poincaré* 2 (2001) 605–673.
- [35] J. Atai, Y. Chen, J. Soto-Crespo, Stability of three-dimensional self-trapped beams with a dark spot surrounded by bright rings of varying intensity, *Phys. Rev. A* 49 (1994) 3170–3173.
- [36] L. Bergé, C. Gouédard, J. Schjodt-Eriksen, H. Ward, Filamentation patterns in Kerr media vs. beam shape robustness, nonlinear saturation and polarization states, *Physica D* 176 (2003) 181–211.
- [37] M. Feit, J. Fleck, Beam nonparaxiality, filament formation, and beam breakup in the self-focusing of optical beams, *J. Opt. Soc. Amer. B* 5 (1988) 633–640.
- [38] G. Fibich, B. Ilan, Vectorial and random effects in self-focusing and in multiple filamentation, *Physica D* 157 (2001) 112–146.
- [39] K. Konno, H. Suzuki, Self-focusing of a laser beam in nonlinear media, *Phys. Scripta* 20 (1979) 382–386.
- [40] J. Soto-Crespo, D. Heatley, E. Wright, N. Akhmediev, Stability of the higher-bound states in a saturable self-focusing medium, *Phys. Rev. A* 44 (1991) 636–644.
- [41] T.D. Grow, A.A. Ishaaya, L.T. Vuong, A.L. Gaeta, N. Gavish, G. Fibich, Collapse dynamics of super-Gaussian beams, *Opt. Express* 14 (2006) 5468–5475.
- [42] W. Ren, X. Wang, An iterative grid redistribution method for singular problems in multiple dimensions, *J. Comput. Phys.* 159 (2000) 246–273.
- [43] G. Fibich, W. Ren, X. Wang, Numerical simulations of self focusing of ultrafast laser pulses, *Phys. Rev. E* 67 (2003) 056603.
- [44] D. Wang, X. Wang, A three-dimensional adaptive method based on the iterative grid redistribution, *J. Comput. Phys.* 199 (2004) 423–436.
- [45] G. Fibich, Self-focusing in the nonlinear Schrödinger equation for ultrashort laser-tissue interactions, Ph.D. Thesis, Courant Institute, NYU, 1994.
- [46] A. Dubietis, G. Tamošauskas, G. Fibich, B. Ilan, Multiple filamentation induced by input-beam ellipticity, *Optim. Lett.* 29 (2004) 1126–1128.
- [47] M. Weinstein, Modulational stability of ground states of nonlinear Schrödinger equations, *SIAM J. Math. Anal.* 16 (1985) 472–490.